Volume 12
Number 13
7 July 2024
Pages 3241-3472

Biomaterials Science

rsc.li/biomaterials-science

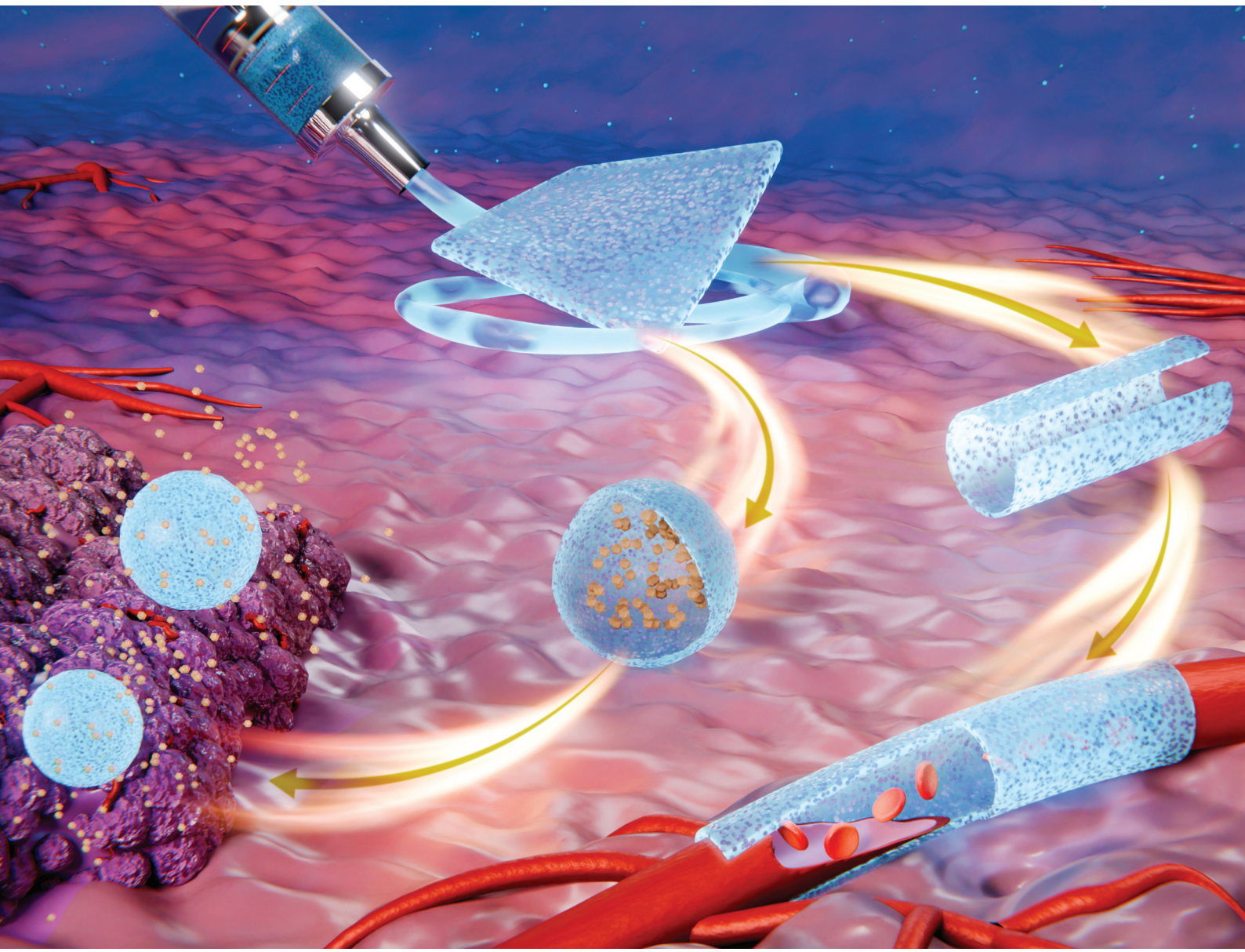

ISSN 2047-4849

ROYAL SOCIETY OF CHEMISTRY

REVIEW ARTICLE
Amit Nain, Souvik Debnath *et al.*
4D hydrogels: fabrication strategies, stimulation mechanisms, and biomedical applications

European Society for Biomaterials

Biomaterials Science

ROYAL SOCIETY OF CHEMISTRY

REVIEW

View Article Online
View Journal | View Issue

Cite this: *Biomater. Sci.*, 2024, **12**, 3249

4D hydrogels: fabrication strategies, stimulation mechanisms, and biomedical applications

Amit Nain, *[a] Srishti Chakraborty,[a] Nipun Jain,[a] Saswat Choudhury,[b] Suravi Chattopadhyay,[a] Kaushik Chatterjee [a,b] and Souvik Debnath *[a]

Received 14th December 2023,
Accepted 14th April 2024

DOI: 10.1039/d3bm02044d

rsc.li/biomaterials-science

Shape-morphing hydrogels have emerged as a promising biomaterial due to their ability to mimic the anisotropic tissue composition by creating a gradient in local swelling behavior. In this case, shape deformations occur due to the non-uniform distribution of internal stresses, asymmetrical swelling, and shrinking of different parts of the same hydrogel. Herein, we discuss the four-dimensional (4D) fabrication techniques (extrusion-based printing, dynamic light processing, and solvent casting) employed to prepare shape-shifting hydrogels. The important distinction between mono- and dual-component hydrogel systems, the capabilities of 3D constructs to undergo uni- and bi-directional shape changes, and the advantages of composite hydrogels compared to their pristine counterparts are presented. Subsequently, various types of actuators such as moisture, light, temperature, pH, and magnetic field and their role in achieving the desired and pre-determined shapes are discussed. These 4D gels have shown remarkable potential as programmable scaffolds for tissue regeneration and drug-delivery systems. Finally, we present futuristic insights into integrating piezoelectric biopolymers and sensors to harvest mechanical energy from motions during shape transformations to develop self-powered biodevices.

1. Introduction

Shape morphing is a nature-inspired critical process in biological systems for the survival of organisms.[1] For instance, several plants such as mimosa, Venus flytrap, and pinecones undergo a shape change in response to environmental stimuli (*e.g.*, humidity, light, and touch) to adapt to ever-changing complex environments.[2] Dynamic shapes can be observed due to the anisotropic tissue composition and random orientation of micro- and nanostructures within the cell. Deformations typically arise from the out-of-plane and in-plane gradient created due to differences in local swelling behavior, amplifying the internal stresses under external stimuli.[3] Therefore, special attention is provided to developing man-made nonliving materials capable of mimicking the behaviors perfected by nature over centuries.[169] In the past decades, shape-morphing materials such as liquid crystal elastomers, shape-memory polymers, and hydrogels have been widely exploited.[4,5] Among these, hydrogels have emerged as one of the most promising candidates.[6] Hydrogels are a class of three-dimensional (3D) interconnected networks comprised of hydrophilic polymer chains.[7] They swell and shrink in response to external stimuli, including pH, light, temperature, ions, and electric and magnetic fields.[8,9]

However, despite these advantages, dynamic behavior is difficult to realize in hydrogels due to their fragile nature. The deployment and implantation of static 3D hydrogels are inconvenient in surgical sutures, posing a high risk of additional complications and severe infection and inflammation at/around the injured tissue site.[10,11] 4D hydrogels offer significant advantages compared to traditional 3D hydrogels. For example, their dynamic adaptability allows them to mimic living tissue, which can support cell growth, guide tissue development, and adjust their shape, structure, and properties to constantly evolving environmental conditions more effectively than static materials.[12] Further, engineered 4D hydrogels pave the way for designing smart materials and devices with tailored responses to different stimuli (pH, moisture, light, *etc.*). Four-dimensional (4D) hydrogels offer precise control of the timing, magnitude, and duration of their responses to external stimuli. This level of control allows researchers to fine-tune the properties of materials and manipulate the behavior of hydrogels with high precision, facilitating their applications in biomedical research and clinical therapies. The versatile nature of 4D gels allows customization to meet the specific requirements of different applications, ranging from tissue engineering and drug delivery to soft robotics. Overall, 4D hydrogels represent a significant step forward in biomaterials science, offering unprecedented control and versatility for

[a]*Department of Materials Engineering, Indian Institute of Science, Bangalore, Karnataka 560012, India. E-mail: amitnain@iisc.ac.in, souvikd@iisc.ac.in*
[b]*Department of Bioengineering, Indian Institute of Science, Bangalore, Karnataka 560012, India*

various applications. Therefore, efforts have been devoted to developing multiple pathways to prepare shape-morphing hydrogels and achieve dynamic architectures.

4D fabrication refers to 3D structures that undergo shape changes in response to certain stimuli with time.[13] These shape transformations are typically governed by a non-uniform distribution of internal stresses, resulting from asymmetrical swelling/shrinking of different parts of the same hydrogel system.[14] 3D printing is the most utilized technique for manufacturing 4D structures,[15] which can be broadly categorized into two types, *i.e.*, direct ink-writing and light-based printing. In this review article, one of each category, *i.e.*, extrusion printing and dynamic light processing (DLP), will be meticulously discussed as an example to shed light on the unique process of developing 4D biomaterials.[15] Extrusion-based 3D printing utilizes a stereolithography file to create G-Code, providing precise control over the structure and predetermined final shape.[16] Alternatively, DLP printers employ projected light sources to cure the complete layer at once.[17] DLP printing was chosen over other light-assisted additive manufacturing techniques (stereolithography, two-photon polymerization, direct-laser writing, *etc.*) because it offers advantages such as high speed, resolution, scalability, material compatibility, customization, and printing capability.[17] Both printing technologies have been reported to produce multidimensional dynamic constructs using two or more component systems to create a gradient between the layers.[18] To date, only a few recent reports have highlighted that the solvent casting method is also capable of producing these dynamic structures by employing a single material.[19] Therefore, we also chose the solvent casting fabrication technique as one of the key highlights of this article. Air drying at an ambient temperature is reported to create sparsely and densely cross-linked regions, leading to spontaneous anisotropic structures.[20] Owing to this nature-inspired route, these 3D constructs show reversibility, making them ideal candidates to be explored in soft robotics.

Shape-morphing hydrogels are in high demand due to their dynamic nature. For example, 3D-printed constructs capable of forming tube-like structures have been explored as nerve conduits to repair peripheral nerve injuries.[21] Compared to the rigid 3D design, a shape-shifting construct exhibited more significant neuronal development due to its conductive and optoelectronic properties.[22] Particularly, by incorporating stimuli-responsive components into the hydrogel matrix, such as proteins or peptides that mimic the extracellular matrix, 4D hydrogels can provide dynamic guidance cues for regenerating nerve cells.[22] In addition, dynamic but controlled degradation prevents risks of inflammation and fibrosus and promotes seamless integration with the surrounding tissues. Moreover, the use of 4D hydrogels facilitates precise control over the spatiotemporal presentation of bioactive molecules, growth factors, and cell adhesion peptides within the nerve conduit. In another study, light-induced gradient cross-linking in a 3D printed polymer network yielded a biomimetic patch, encouraging cardiomyocyte maturation and vascularization to promote cardiac regeneration.[23] Similar to the nervous system, the heart is also a dynamic organ that experiences continuous mechanical forces. 4D hydrogels are designed to dynamically adjust their mechanical properties in response to variations in pressure or stretching. This dynamic behavior helps mimic the natural mechanical cues experienced by cardiac cells, promoting their alignment, maturation, and functionality within the engineered tissue. Moreover, an advanced drug delivery platform can be created using a 4D fabrication approach, allowing exact control over administered medicines, biomolecules, and cells in a programmed manner. Drug release can be actuated by various stimuli such as temperature, selective enzymes, pH, and humidity/moisture.[24] However, it is challenging to achieve and maintain the ideal temperature for drug release, and dramatic changes in pH often contribute to the rapid degradation of the scaffold.[25] Furthermore, although moisture is a cell-friendly stimulation, achieving complete deformation at the superficial tissue site, such as skin, is difficult due to its higher dehydration rate.[26] Nevertheless, despite these challenges, shape-shifting biomimetic hydrogels have gained attention from the scientific community, which is evident from the literature published in the past seven years.[27]

Several years ago, Furukawa and group summarized the literature on shape-memory hydrogels and their potential application in soft robotics.[28] Similarly, a review article on shape-morphing hydrogels was published last year by Liu *et al.*,[29] highlighting the utility of shape-morphing characteristics in grippers, sensors, valves, soft robotics, and other mechanical applications.[29] Therefore, an article highlighting the potential of programmable and dynamic hydrogels in the biomedical field was lacking. In this case, Dong *et al.* published an article on 4D printed hydrogels, discussing their fabrication strategies, materials, and applications in actuators and drug delivery.[30] In the same year, Champeau *et al.* provided a comprehensive review on the state-of-the-art of 4D printing technology for the fabrication of shape-morphing hydrogels.[31] However, although these articles were well drafted from a materials perspective, there have been several new developments in the past five years. Furthermore, these papers only focused on 3D printing technology, while other methods such as solvent casting have been employed to prepare 4D hydrogels. In addition, an in depth discussion on the utility of these hydrogels in bioengineering is still missing. Thus, in this review, we aim to provide a compressive discussion on various 4D fabrication techniques, including extrusion-based 3D printing, DLP, and solvent casting, and their application in stimuli-triggered complex tissue engineering and drug delivery. While discussing these innovative methods, an important distinction between mono- and dual-component, uni- and bi-directional shape change, and pristine and composite hydrogel systems is made. Herein, we also highlight the distinctive features of shape-morphing hydrogels that help produce intricate scaffold designs such as tubes that can serve as potential grafts, stents, or conduits. Furthermore, we present comparative arguments that will provide better readability and understanding of shape-morphing systems in tissue engineering and drug deliv-

ery applications. Subsequently, we summarize the importance of this emerging class of biomaterials and identify opportunities for the future. Finally, we discuss the potential of integrating electrical components and sensors within the dynamic structures that can revolutionize regenerative engineering. Rapid growth in the biomaterial domain and the capabilities of data science to create imaginative tools and techniques based on artificial intelligence and deep-learning algorithms can widen the field of biorobotics.

2. Types of 4D fabrication techniques

Hydrogels are gel-like substances and belong to a class of soft materials, which are capable of absorbing and retaining large amounts of water. These networks of gels can be prepared *via* physical or chemical crosslinking of polymer chains to form a stable matrix, which can be tailored to control mechanical strength, porosity, and other physicochemical properties. Hydrogels exhibit stimuli responsiveness depending on the formulation strategy and choice of polymer. Additionally, 3D hydrogels undergo shape morphism to produce more complex designs and shapes, also known as four-dimensional (4D) fabrication.[32,33] There are multiple actuators that can drive shape morphism within hydrogels, such as pH, temperature, light, and ions.[34–36] In the case of 4D fabrication, hydrogel structures can change their shape or properties over time in response to environmental cues, making them attractive for tissue engineering, drug delivery, and soft robotics applications. Below, we discuss the various strategies for preparing stimuli-responsive hydrogels. We also highlight the influence of composition, structural anisotropy, and formulation strategies on the shape-morphism of the fabricated hydrogels.

2.1. Extrusion-based 3D printing

One of the fabrication techniques to achieve shape-morphing hydrogels is 3D printing. 3D printing has emerged as transformative technology in shape morphing, revolutionizing the design and creation of objects that can change their physical form. 3D printing is pivotal in advancing the capabilities of shape-morphing technology, ushering in a new era of design and engineering possibilities in the development of self-assembling structures for aerospace, adaptable medical implants, and shape-shifting architectural elements.[37–39] 3D printing enables the production of intricate structures with embedded materials that respond to external stimuli, such as pH, ions, and light, to alter their shape.[40] 3D printing enables the inhomogeneous incorporation of multiple components within the hydrogel, leading to different properties that contribute to variable swelling and attractive shape-morphing patterns, making it a desirable technique for 4D fabrication.[41] Some of the most widely used forms of 3D printing include direct-ink writing (DIW), digital light processing (DLP), stereolithography (SLA), fused deposition modeling, two-photon polymerization (TPP), and ion-inkjet-printing (IIP).[42] In the typical 4D fabrication of hydrogels, one or more components are employed and designed to generate gradient cross-linking, which enables shape change in the printed structures. Firstly, we discuss dual-component hydrogel systems. In another report, Joshi *et al.* created a dual-component hydrogel system comprised of alginate and methyl cellulose through extrusion-based 3D printing to develop a self-rolling nerve conduit.[43] Two different gels of high (3 : 9) and low (4 : 6) porosity were synthesized by adjusting the composition of alginate and methylcellulose (Fig. 1A). Two consecutive layers of 4 : 6 were extruded onto a 3 : 9 gel (bottom layer) in the form of strips and placed at 0°, 45°, and 45° angles with respect to the base layer to have precise control of the shape-deformation. Shape change occurred when the air-dried structures were immersed in calcium chloride solution due to chemical cross-linking.[21] The direction of bending or twisting in the gel could be precisely anticipated and corroborated through computational simulations. Together with a pre-determined CAD design, the infill angle and differential cross-linking between the bottom and top layers were crucial for observing shape-morphism in a dual-component hydrogel system. In another dual-component system, Mao *et al.* developed a chitin-polydimethylsiloxane (PDMS) hydrogel capable of producing complicated multidimensional architectures.[44] PDMS ink containing 90% pre-polymer and 10% curing agent was printed onto chitin film prepared by treating chitin (4 g) with sodium hydroxide (11%) and urea (4%). PDMS strips were3D printed on the chitin film (Fig. 1B) and the printed constructs were cured at 150 °C. Various structures were created by programming twelve components with different printing angles and interlayer spacing, followed by heat treatment and cutting. The actuation speed depended on the thickness of the structures and the shape reversibility was controlled by ethanol. The rapid response in water/ethanol solutions resulted from the significant modulus difference between the chitin film and PDMS, minimizing the swelling, and the hydrophobic nature of the PDMS layer, ensuring stable force and outperforming other dual-component hydrogel systems.

Alternatively, mono-component hydrogel systems have also been demonstrated. However, unlike dual component hydrogel systems, shape-change due to swelling gradient, infill pattern, and infill angle between the two layers are difficult to achieve employing only one material. Lai *et al.* printed multiple layers of alginate-based ink, which, apparently on-air drying, formed varying intra-structure network densities (dense and sparse region), leading to anisotropic swelling and controlled shape morphing upon chemical cross-linking. Similar to a dual-component system, a solid bottom and patterned top layers were printed using the same hydrogel ink instead of two.[45] The gel was printed at ~2.5–3 bar, with a layer thickness of 0.2 mm, at the rate of 8 mm s^{-1} through a 22G nozzle. Recently, Ghosh and group demonstrated the development of a shape-morphing mono-component system using a customized DIW printer.[46] The chitosan-based ink could print at 5 bars through a nozzle (diameter: 500 μm) at the rate of 5 mm s^{-1}, and the printed structures were cross-liked *via* thermal curing (150 °C, 10 min). The authors observed shape-morphism in the printed

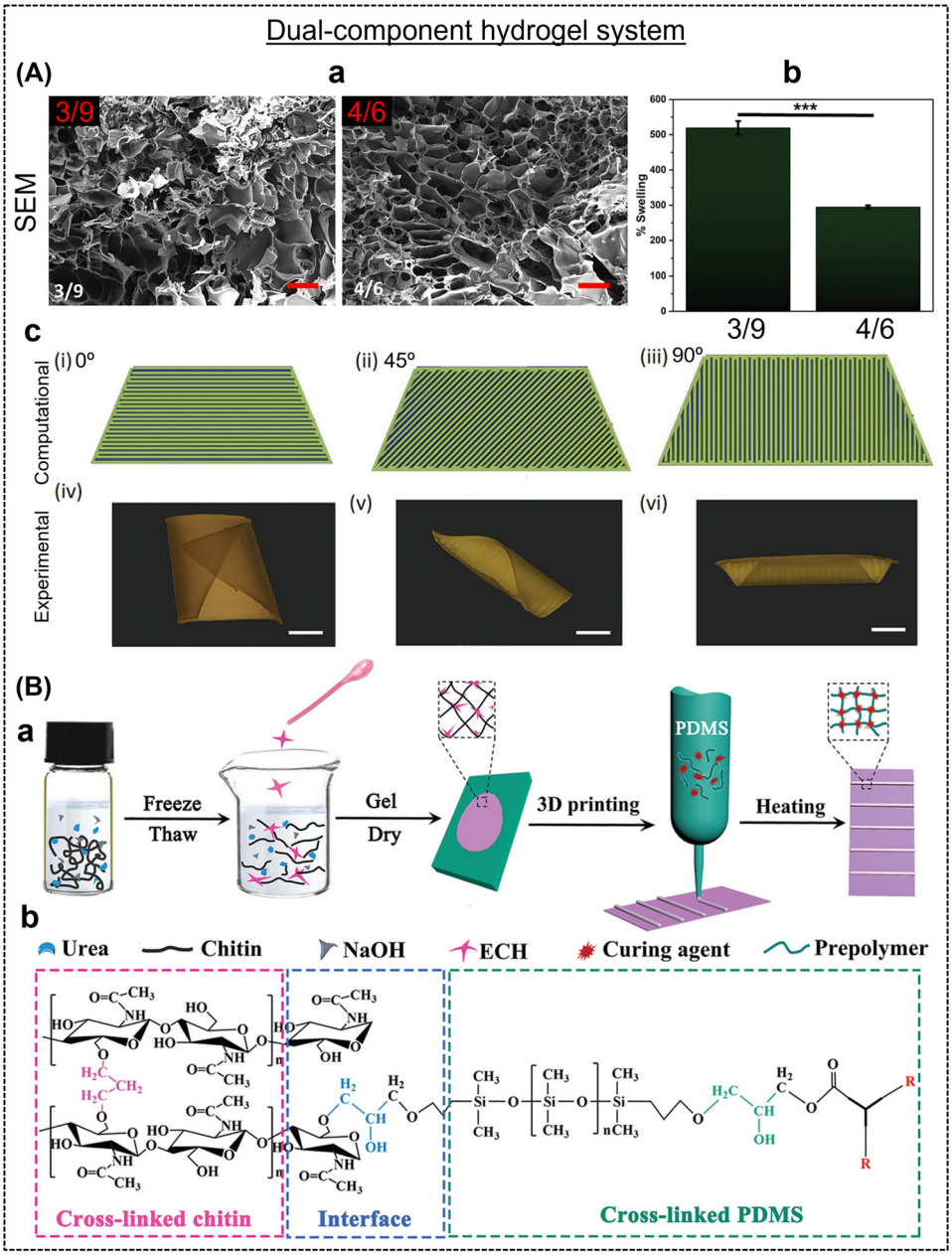

Fig. 1 (A) (a) SEM images and (b) % swelling of two different types of gels. Computational prediction and experimental validation of various modeled G-codes and real-time photographs of the deformed gels in the presence of Ca^{2+}. Scale bars are 12 mm. Reproduced with permission.[21] Copyright 2023, Wiley Online Library. (B) Fabrication and chemical cross-linking process of shape-shifting actuators developed using chitin/PDMS composite. Reproduced with permission.[44] Copyright 2020, Wiley Online Library.

structure only when one side of the chitosan film was exposed to the solvent. This dynamic behavior of the chitosan structure was not demonstrated upon complete immersion, which is mainly due to the net-zero concentration gradient across the film. The reported hydrogel was employed as a gripper to lift objects seven times its weight.

Shape-morphing is an attractive feature of a material; however, to date, most of the published reports showed uni-directional shape-morphism. It is a challenge to create multi-directional or reversible actuators. In this case, our group reported a the fabrication of a hydrogel with a humidity-responsive interpenetrating network, which was capable of changing its shape in more than one direction due to gradient photo-crosslinking and anisotropic water absorption (Fig. 2A).[43] The hydrogel ink was comprised of methacrylated carboxy-methyl cellulose, a photoinitiator (lithium phenyl-2,4,6-tri-methylbenzoylphosphinate), and methylcellulose. During the process of photocrosslinking, the gradual reduction in light intensity as it penetrates deeper into the material results in a spatial gradient of cross-linking density throughout the thick-

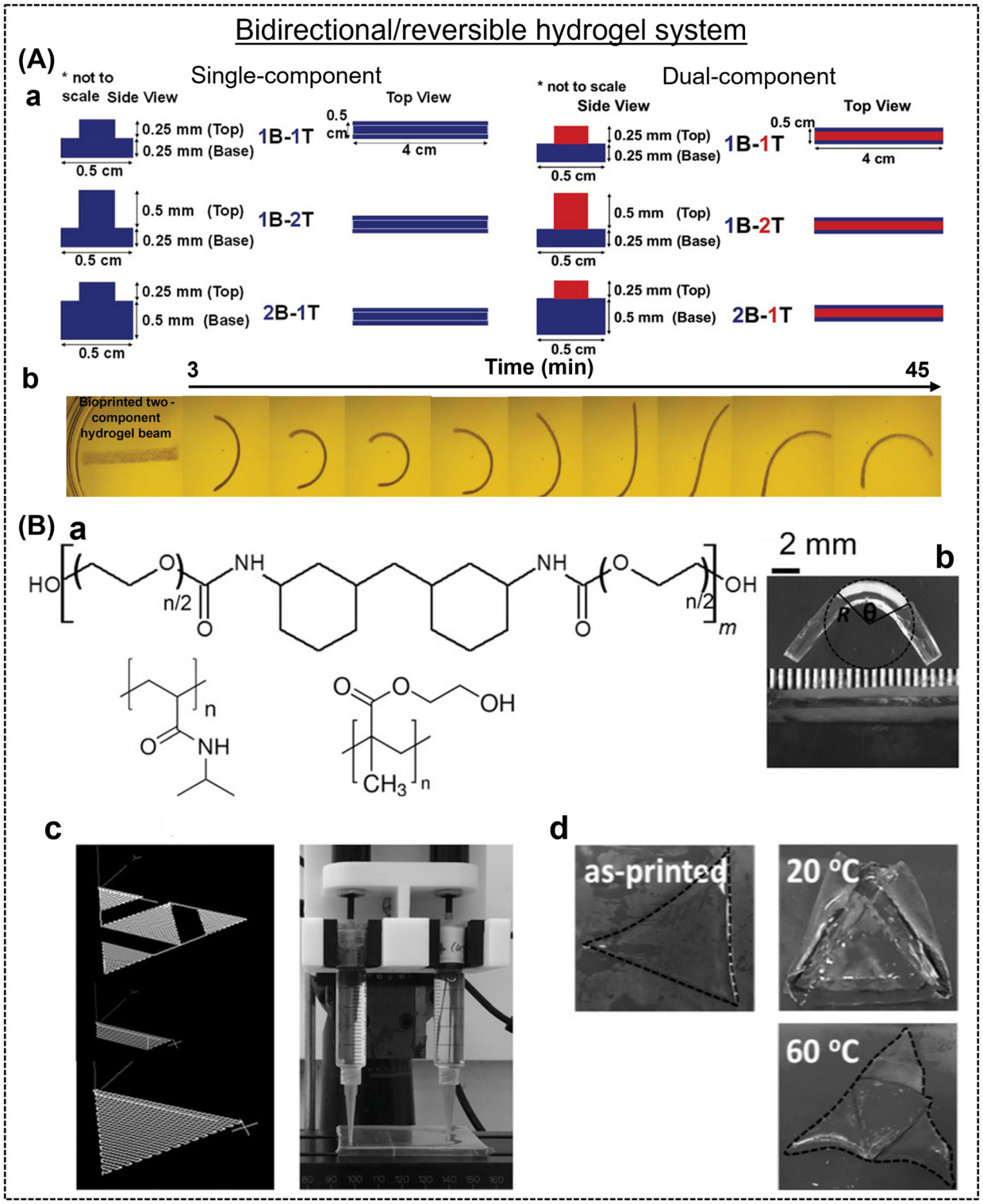

Fig. 2 (A) (a) 4D hydrogel fabrication process and (b) bi-directional shape-morphing features of single- and dual-component hydrogel systems. Reproduced with permission.[43] Copyright 2023, Wiley Online Library. (B) (a) Extrudable inks prepared using polyether-based linear polyurethane, poly(NIPAM), and poly(HEMA), (b) bilayer hinges in a deformed state, (c) hydrogel printing process and its design, and (d) real-time images of printed hydrogels at different temperatures. Reproduced with permission.[47] Copyright 2016, Wiley Online Library.

ness of the hydrogel, leading to the upper portion receiving more intense exposure to the incoming irradiation, and consequently forming a higher degree of cross-links compared to the lower portion. After the hydrogel beam was submerged in deionized water, this gradient in photo cross-linking led to uneven swelling within the beam, resulting in rapid bending

into a ring shape. As discussed above, Ghosh and group also highlighted the solvent-actuated reversibility in chitosan-based hydrogels, which is probably due to the limited solubility of chitosan in ethanol, which led to the contraction of the polymer chains.[46] Moreover, Mao *et al.* commented on the reversibility of the printed structures in a water/ethanol system. The bidirectional shape morphism is truly a unique phenomenon.[44] In another report, Naficy *et al.* demonstrated temperature-induced reversible or bidirectional shape-morphism in a photo cross-linked poly(NIPAM) and poly(HEMA) bilayer hydrogel.[47] The bilayer hydrogel flat sheets underwent shape morphism when they became fully swollen at temperatures below 32 °C and reverted to their flat state when the temperature exceeded 32 °C (Fig. 2B). The thickness and length of the printed materials were two crucial parameters to achieve reversibility.

2.2. Dynamic-light processing

DLP is an alternative printing method to create shape-morphing hydrogels; however, there have been few reports on this topic thus far. The first report by Zhao *et al.* explored the feasibility of designing intricate wettability behavior-induced shape-shifting structures.[48] An innovative composite comprised of a hydrophilic layer (polyethylene glycol diacrylate; PEGDA) that swells in water and a hydrophobic coating (poly (propylene glycol) dimethacrylate; PPGDMA) providing structural support was fabricated with sequential actuation behavior using a DLP projector (Fig. 3A). Instead of relying on intricate photomasks, the polymer structures were generated by illuminating predefined grayscale images, either in a single-step or multi-step manner. A mismatch in strain was induced by fixing hydrophilic PEGDA rubber on both sides of the hydrophobic PPGDMA sheet to achieve shape change. Eventually, the DLP-processed flat sheets were immersed in water, leading to equilibrium swelling and attaining their final shapes. For example, non-uniform bending and subsequent out-of-plane buckling of a ring-shaped plate transformed into a wavy ring. DLP technology offered the advantage of seamlessly introducing a light intensity gradient into the illumination patterns, facilitating complex shape transformations. Based on a similar technique, our group formulated a humidity-responsive photopolymerizable bio-ink to print shape-morphing adult human tissue.[49] The bioink featured cell-adhesive Arg-Gly-Asp (RGD) peptide sequences rich in methacrylated gelatin (GelMA) and PEGDM to provide cell support and mechanical integrity to the printed structures, respectively. DLP processing involved the use of visible light (405 nm)-responsive photoinitiators, specifically lithium phenyl-2,4,6-trimethylbenzoylphosphinate, and a photoabsorber, tartrazine (Fig. 3B). The first two layers of the bio-ink, each having a thickness of 100 μm, were exposed to a consistent curing time of 56 s, while the subsequent layers received a shorter curing time of 14 s. Subsequently, these sheets were extracted from the build plate and immersed in water for 2 h to observe their shape change. Tartrazine governed the depth of curing in the layer-by-layer printed structures, thereby imparting a gradient in cross-linking across the construct.

In recent times, the realm of grayscale curing has been extended to DLP-based printing by Kuang *et al.*[50] They developed a hybrid ink containing bisphenol A ethoxylatediacrylate (BPADA), glycidyl methacrylate (GMA), *n*-butyl acrylate (BA), a diamine cross-linker [poly(propylene glycol) bis(2-aminopropyl ether); D230], photoinitiators (Irgacure 819) and photoabsorbers (Sudan I). In single-vat g-DLP 3D printing, grayscale images, representing the light intensity in monochrome mode, were employed to solidify the resin layer-by-layer selectively. The desired structure was initially divided into images corresponding to individual printing layers. These images were processed using a MATLAB code to create grayscale distributions based on the desired properties. Subsequently, a UV projector was employed to print each layer with grayscale patterns. Initially, the acrylates underwent radical-induced photopolymerization, forming a polymer network that defines the shape of the printed part. The cross-linking density and modulus of a material decrease as the grayscale percentage increases. Following a desolvation treatment in a water/acetone solution (15 : 1 v/v), the compact 3D-printed flower transformed into a fully blossomed state, triggered by the contraction of the outer layer of each petal. Subsequently, when treated with acetone, the blossomed flower reverted to its original un-blossomed form, driven by the swelling disparity between the outer layer with a lower cross-linking density and the inner layer with a higher cross-linking density. This reversible shape-shifting process continued to occur iteratively as acetone was absorbed, and subsequently evaporated. In another study by Roach *et al.*, a 4D-printed composite material composed of LCE and SMP was developed.[51] The printed material showed rapid and reversible shape changes, while retaining a mechanical stiffness of approximately 1 GPa in its actuated state (Fig. 3C). Shape changes were triggered by the thermo-mechanical properties of LCE and SMP, which depended on the cooling rate. Specifically, varying cooling rates allowed the composite to assume different shapes, while maintaining high stiffness at lower temperatures (Fig. 3C-d). A multi-material 4D printing approach was utilized to construct a bilayer composite, where SMP and LCE were printed using the DLP and DIW techniques, respectively. This novel approach opens the door to potential applications in various fields, including space exploration, biomedicine, soft robotics, and energy technologies.

2.3. Solvent casting

Solvent casting is a facile alternative to the abovementioned additive manufacturing techniques; however, it is rarely explored for 4D fabrication due to the lack of control over the internal structures. Briefly, a dissolved polymer solution solidifies *via* the evaporation of the solvent in a mold of the desired shape and size.[52] Solvent casting can offer a unique approach to creating dynamic materials. Unlike 3D printers, where the fidelity of the ink is critical to the process, solvent casting is versatile and suitable for most polymers. In addition, the cost

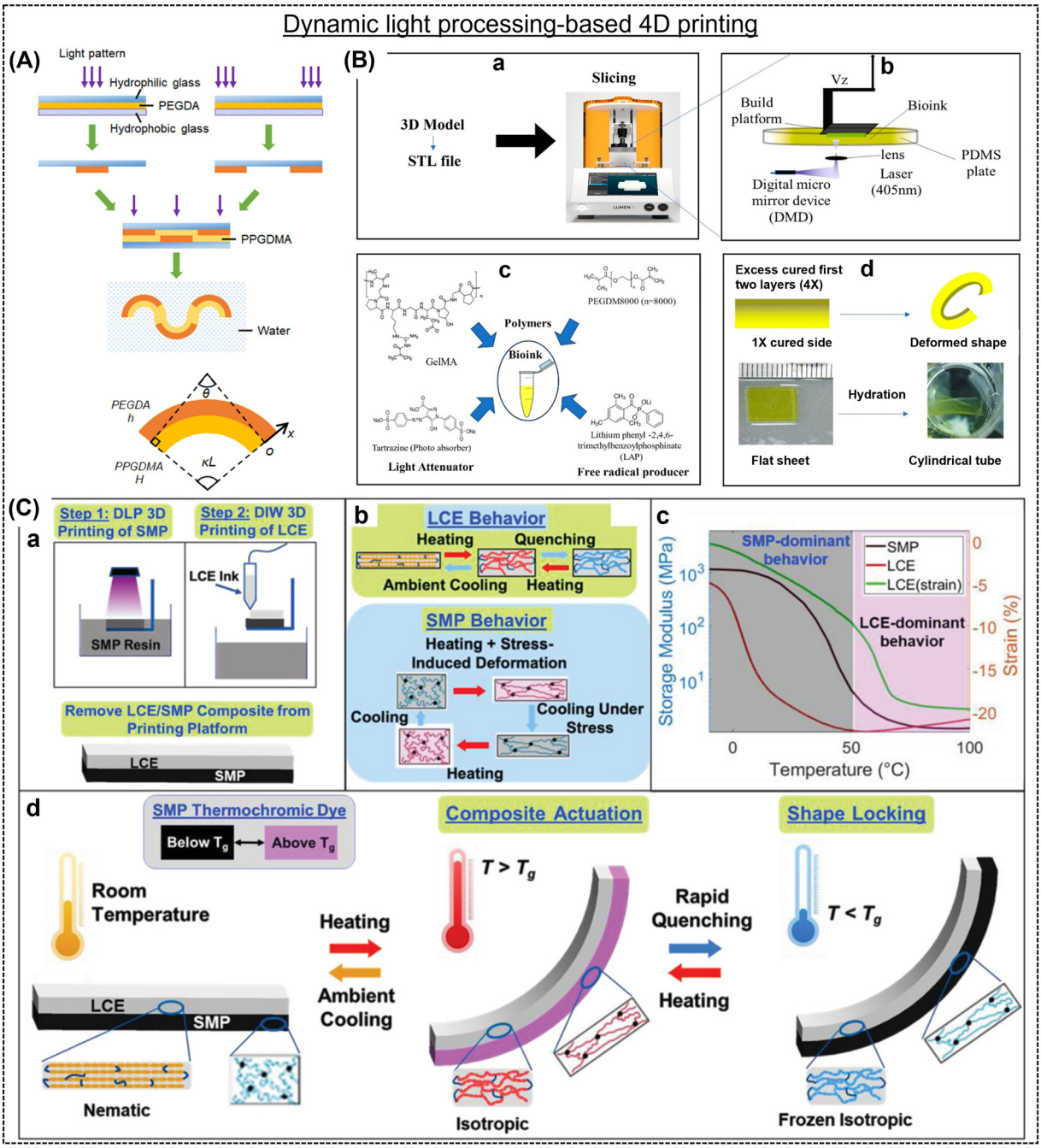

Fig. 3 (A) Schematic representation of the hydrophilic/hydrophobic composite hydrogel preparation and shape-morphing feature. Two independent PEGDA patterns were cross-linked using different light, and subsequently the hydrophilic glass was removed from the hydrophobic glass. Two PEGDA patterns were assembled and injected with PPGDMA liquid resin to cure the whole structure. Reproduced with permission.[48] Copyright 2018, ACS. (B) 4D Bioprinting of P2G12.5 Bioink in Cell Culture Media and structural deformations after hydration. Reproduced with permission.[49] Copyright 2023, ACS. (C) Schematic representation of (a) two-step 3D printing (DLP&DIW), (b) thermomechanical behavior, (c) storage modulus curves, and (d) shape-transformation of the LCE and SMP composites. Reproduced with permission.[51] Copyright 2022, Wiley Online Library.

of a 3D printer and harboring skilled manpower are significant, while solvent casting only requires a container and precursor. As discussed above, shape transformation is often a result of gradient crosslinking, which is generated carefully by printing one or more materials in a way that their different swelling behaviors and porosity can be exploited. On the contrary, solvent casting involves the drying of the solvent. If the reaction occurs at room temperature, a natural intra-structural gradient is created due to the depth of the solution, subsequently triggering shape-morphism in response to moisture. For example, Hu *et al.* reported a solvent casting method to produce a chitosan hydrogel film (mono-component) capable

of shape-transformation due to the gradient crosslinking and geometry effect created by the top-down diffusion of glutaraldehyde molecules within a chitosan pre-gel solution (Fig. 4A).[36] The chitosan film forms tight networks (densely cross-linked) at the top surface owing to complete exposure to the glutaraldehyde solution.[53] In contrast, the bottom surface was only sparsely cross-linked due to the inability of glutaraldehyde to penetrate the deeper sites. The formation of dense-sparse networks within the structure was validated by the variation in pore size and Young's modulus value (Fig. 4A-b). In the report by Guo *et al.*,[54] they showed that even air-dried 3D printed structures can undergo shape-morphing due to the naturally created anisotropy within the films. Poly(stearyl acrylate-*co*-acrylic acid) (P(SA-*co*-AAc)) dissolved in ethanol was extruded onto a substrate, then allowed to partially solidify through solvent evaporation in the air, and subsequently subjected to solvent exchange in water to create gel constructs with altered morphologies. The differences in swelling properties induced a transformation in the gel structures. Solvent casting fabrication techniques, though rare, have still been found in the literature to develop shape-shifting structures, mainly using air-drying techniques. By carefully controlling this crosslinking gradient, engineers and researchers can manipulate the response of a material to external stimuli.[55]

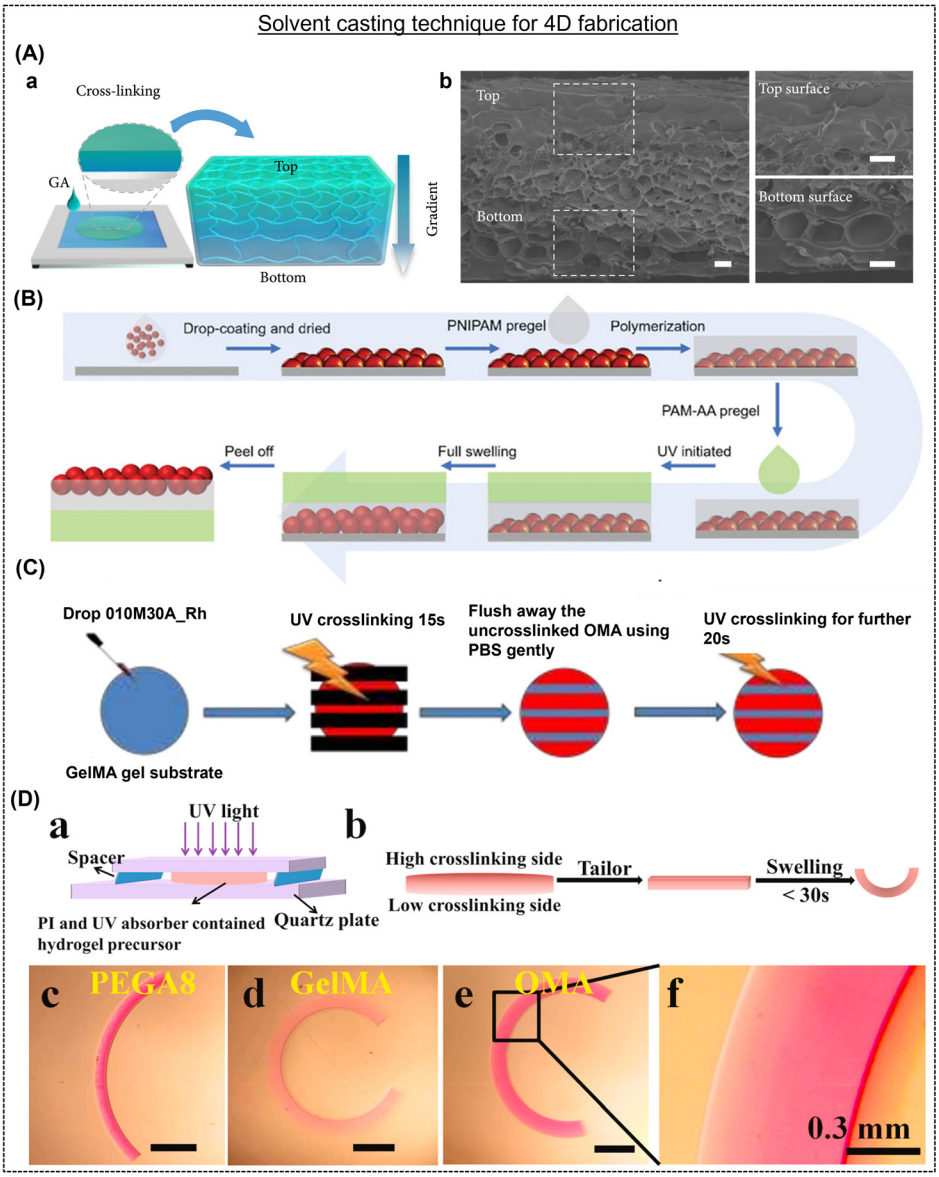

Fig. 4 (A) Schematic representation indicating gradient cross-linking density within the chitosan hydrogel films. Reproduced with permission.[36] Copyright 2021, Science. (B) Fabrication process of a hydrogel with structural and shape change properties. Reproduced with permission.[56] Copyright 2022, Wiley Online Library. (C) Schematic illustration of patterning OMAs onto a single GelMA. Reproduced with permission.[57] Copyright 2021, Wiley Online Library. (D) (a and b) Typical experimental setup to prepare hydrogel with differential gradients and (c–f) microscopic images of various hydrogels after swelling. Reproduced with permission.[58] Copyright 2022, Elsevier.

This innovative approach involves selectively varying the degree of crosslinking within a material, creating a gradient in its stiffness or rigidity. Shape-morphing materials designed by air drying typically rely on moisture absorption or desorption as their triggering mechanism. Therefore, their structure may gradually return to its original state upon dehydration.

Yu *et al.* employed a process to fabricate reversible grippers involving the fabrication of a bi-layered structure comprised of poly(*N*-isopropylacrylamide) (PNIPAM) and inert poly(acrylamide–acrylic acid).[56] The multi-step fabrication technique involved the synthesis of a thermos-responsive poly(*N*-isopropylacrylamide-*co*-styrene) (PNIPAMST) microgel emulsion through surfactant-free precipitation polymerization, followed by the preparation of the PNIPAMST microgel film by coating it onto a glass coverslip and obtaining a dry film, and then the fabrication of a PNIPAM pregel by dissolving its precursors in deionized water (Fig. 4B). A dried PNIPAMST microgel film was used as the base, onto which NIPAM solution was casted, followed by AM-AA/multi-walled carbon nanotube (MWCNT) dispersion, resulting in a bilayer hydrogel that was shaped into a flower and tested for its flexibility using varying thickness ratios and lengths in the absence of the PNIPAMST microgel layer. The structure could successfully replicate the function of an octopus, together with having the properties of tunable color and shape under the influence of a temperature stimulus. The near infrared (NIR)-active MWCNTs also contributed the added benefit of the flower structure blooming or opening up upon irradiation.

In another report, Ding *et al.* demonstrated a natural polymer-based hydrogel system capable of "on-demand", multiple, and reversible shape-morphing due to multilayered oxidized methacrylated alginate (OMA) and GelMA hydrogels (Fig. 4C).[57] The facile fabrication method involved initially UV-crosslinking the OMA hydrogel, followed by crosslinking the GelMA solution between the OMA layers, thereby offering simplicity, convenience, and adaptability, and consequently facilitating the production of hydrogel actuators with varying levels of complexity. Alsberg's group showed 4D biofabrication using a mono or dual component strategy. A mixture containing polymer (OMA 6% w/v, GelMA 14% w/v, or PEGA8 20% w/v), PI (0.05% w/v), and UV absorber, fluorescein isothiocyanate derivatives, and/or 4′-hydroxy-3′-methylacetophenone in a cell medium in the absence and presence of mammalian cell lines was placed between two quartz plates (with a 0.6 mm spacer) and photo-cross-linked with UV light (20 mW cm^{-2}) for 30 s (OMA), 180 s (GelMA), and 30 s (PEGA8) to fabricate a hydrogel bar (13 mm × 2 mm × 0.6 mm) (Fig. 4D).[58] OMA gel precursors were placed underneath a pre-gelled GelMA layer (30 s UV) and cut into bilayer bars to form bilayered constructs. The hydrogel bars were immersed in an aqueous solution to observe shape-morphing and reached maximal bending in 30 min. This method facilitated the synthesis of large-scale microstructures in a substantially simpler, economical, and quicker way. Utilizing the gradient crosslinking principle, it becomes feasible to intentionally create multiple gradients featuring more than one direction within a single hydrogel framework. Consequently, this method simplifies the generation of intricate structures possessing asymmetric geometries within a monolayer hydrogel.

3. Types of stimulation and their mechanism

Reflecting on the recent advancements in the processing of hydrogels, they are considered a class of "smart" materials by demonstrating programmable shape-morphing behavior upon exposure to various chemical and physical stimuli. Various stimulation strategies exist to drive the shape change in hydrogels, including chemical, physical and biochemical signals.[29] Hydrogels are intrinsically isotropic materials that experience uniform volumetric expansion and contraction in response to suitable stimuli.[1] However, upon careful fabrication, hydrogels can be tuned to exhibit differential swelling by restricting and/or increasing swelling in certain positions or directions in the same structure.[59] Careful generation of anisotropy in the structure of hydrogels will allow them to transform into different shapes immediately after swelling. In this section, we discuss the various stimulation mechanisms that can yield shape morphing in hydrogels.

3.1. Solvent/humidity

The natural phenomenon in hydrogels, *i.e.*, swelling and shrinking, has been leveraged to realize anisotropic swelling-mediated shape morphing.[6] These gels can be smartly sandwiched between passive layers (unresponsive to moisture) to drive out-of-plane motions. For instance, an active layer comprised of a copolymer of PEG and polytetramethylene glycol (PTMG) and an inactive layer of beeswax were stacked on each other, which underwent fast-hygroscopic expansion of the copolymer, leading to the structure bending towards the inactive layer side (Fig. 5A).[60] This phenomenon is due to the swelling differences between the two layers. Another way of generating anisotropy in a structure is to fabricate composites of a soft gel and a stiffer reinforcement. For example, Gladman *et al.* 3D printed a humidity-responsive *N*,*N*-dimethylacrylamide-based matrix incorporated with stiff nanofibrillated cellulose, which caused alignment of the fibrils along the printing path, leading to anisotropic stiffness in the printed part and a curved shape after swelling (Fig. 5A-b).[61] The shape changes were programmable based on the print path, and the final curvature was predicted using modeling. Besides reinforcement-induced anisotropy, different compositions of the same material, which have significant differences in their swelling rates, can be stacked upon each other during 3D printing to drive anisotropic swelling and out-of-plane movements. Our group prepared a dual-component hydrogel system with shape-shifting capabilities.[21] Two gels with profoundly different swelling behaviors in water were prepared by varying the composition of alginate and methylcellulose. Both gels were stacked on each other by extrusion-3D printing, which also controlled the infill angles

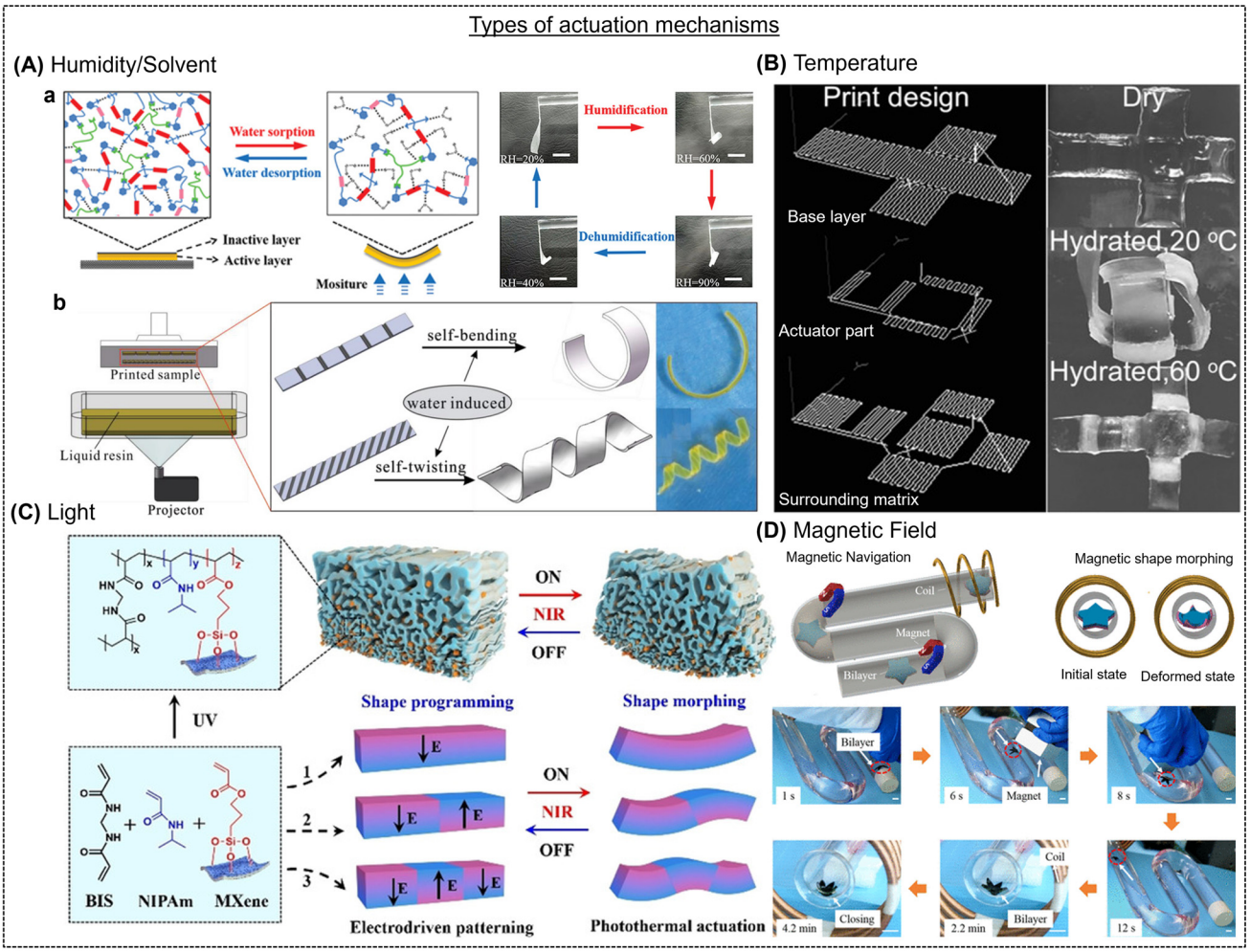

Fig. 5 (A) Humidity/solvent-responsive shape-morphing hydrogels. (A-a) Structural changes in the copolymer comprised of an active (yellow) and inactive (black) layer involving chitosan bonds upon moisture sorption and desorption. Reproduced with permission.[60] Copyright 2019, Wiley Online Library. (A-b) Experimental printing setup (left) and shape-morphing of the 3D-printed construct with pre-programed secondary grooves. Reproduced with permission.[62] Copyright 2019, Wiley Online Library. (B) Three layers of a 3D printed construct, base layer, thermos-responsive part, and a surrounding matrix and their reversible shape-shifting phenomenon in response to temperature. The scale bar is 1 cm. Reproduced with permission.[47] Copyright 2016, Wiley Online Library. (C) Chemical structures, 3D printed materials, electro-driven shape-programming, and light-induced shape-changes in MXene-containing hydrogels. Reproduced with permission.[76] Copyright 2020, Wiley Online Library. (D) Navigation and shape morphing of a star-like bilayer in response to an alternating magnetic field. The scale bar is 10 mm. Reproduced with permission.[84] Copyright 2019, ACS.

and density of the top (lower swelling rate) and bottom layer (higher swelling rate). This led to programmable shape changes in a single structure by varying the printing parameters, and theoretical simulations predicted the same. Based on a similar principle, Ji *et al.* showed a one-step 3D printing process to prepare a moisture shape-morphing hydrogel system comprised of polyethylene glycol diacrylate (PEG400DA) and 2-hydroxyethyl methacrylate (HEMA) (Fig. 5A-c).[62] Anisotropy was introduced by the secondary grooves on one side of the structure, which led to either bending or twisting due to local curvatures and asymmetrical swelling. Water is an inert and biocompatible stimulus for triggering the shape morphing of constructs embedded with cells; therefore, it can be leveraged for fabricating complex tissue constructs.[30,63–66] For example, Kirillova *et al.* employed a mixture of methacrylated alginate and methacrylated hyaluronic acid, 3D printed with bone marrow stromal cells, photo cross-linked, and mildly dried.[67] The crosslinking gradient induced by the top layer by absorbing more light than the bottom, bioprinted constructs exhibited instant self-folding into tubes with the cells distributed evenly along the walls of the formed tube Although. However, although moisture/solvent is a natural and benign actuation method, a key bottleneck remains to be resolved, *i.e.*, the long-term stability of the formed constructs *in vivo* and their performance in tissue regeneration.

3.2. Temperature

Changes in temperature, especially in a range compatible with human tissues of ≈36–38 °C, can be an attractive trigger to achieve shape deformations in hydrogels. The temperature-dependent molecular interactions between the polymer chains in a hydrogel and the solvent lead to profound swelling or shrinkage. Thermally responsive hydrogels can exhibit a lower critical solution temperature (LCST) or an upper critical solution temperature (UCST). The LCST hydrogels with negative thermosensitivity are shrunk above their critical temperature, while UCST hydrogels with positive thermosensitivity remain swollen above their critical temperature.[68] Thermoresponsive gel systems are largely dominated by reversible LCST-based hydrogels, and most notably poly(*N*-isopropyl acrylamide) (pNIPAM) and its derivatives.[69] This is due to the large volume changes in pNIPAM at a relatively low LCST temperature of ≈32 °C.[70] For example, Naficy *et al.* developed bilayered hydrogels from thermosensitive pNIPAM and non-active polyHEMA, which could self-morph from a flat shape to controllable 3D structures when the temperature was above 32 °C and back to the flat state when the temperature was below 32 °C (Fig. 5B).[47] This temperature-dependent reversible shape-morphing phenomenon was explained by a simple model that correlates the material and printing parameters with the final 3D structure of the hydrogels.[47] In another report, Xu *et al.* prepared Fe^{3+} ions cross-linked hydrogels from pNIPAM and sodium methyl acrylate monomers to enable complex shape changes, including origami designs.[55] Through the local release of Fe^{3+} ions into the gel network and further periodic crosslinking, the gel exhibited shape deformations into a helix below 50 °C, and the helix deformed above 50 °C, leading to reversible out-of-plane deformations. However, going further, more rapid and complex shape changes need to be designed in hydrogels at temperatures around the physiological range to fulfill a range of biomedical applications.

3.3. Light

Light stimulation has attracted significant interest due to the ability to precisely control its properties, such as wavelength and intensity, and the capability of contactless remote manipulation.[71,72] In contrast to other actuation modes that enable the gel to respond globally, light can trigger specific and localized reconfigurations by irradiating specific regions of the sample.[73] Photoresponsive gels exhibit large volume changes *via* swelling or shrinkage due to water uptake or release, respectively, upon light radiation.[74] The swelling rate of a gel can be tuned by the polymer hydrophilicity and cross-linking density, which can also be manipulated using light. NIR light is preferred for biomedical applications over ultraviolet and visible light due to its higher tissue penetration depth. NIR-triggered shape morphing was explored in alginate-polydopamine cell-laden gels, wherein the initial lamellar structure transformed into a saddle-like shape by gradual dehydration under NIR.[75] In another report, Xue *et al.* employed a photopolymerizable MXene nanomonomer in conjunction with thermosensitive PNIPAm hydrogels to induce a concentration gradient of MXene nanosheets across the thickness of the gel, resulting in a shape change (Fig. 5C).[76] These gels exhibited fast light-driven directional shape morphing due to the photothermal effect of MXene. Other strategies include inserting regions of a light-active composite, *i.e.*, photothermal reduced graphene oxide (rGO) fillers in a thermoresponsive gel, PNIPAm, into a non-responsive matrix, which generates swelling mismatch, and consequently shape change.[77,78] The shape change could be global by immersing the structure in water at 50 °C (above the LCST of PNIPAm) or localized by directing light on a specific region of the strips. One of the major limitations of light-driven shape morphing gels is the small extent of shape change, which limits its application prospects.

3.4. Magnetic field

A magnetic field is a preferred stimulus for driving remote and local shape changes and is biocompatible even at high field strengths.[79,80] Magnetic hydrogels are usually fabricated by reinforcing magnetic fillers, such as iron oxide and cobalt oxide, which can respond to an external magnetic field (MF).[81] Three fundamental fabrication strategies exist for developing magnetic 3D hydrogels, as follows: (a) *in situ* precipitation, (b) blending, and (c) grafting-onto method.[82,83] For instance, Wang *et al.* prepared magnetic hydrogel nanocomposites (also called ferrogels) that can respond to an external MF in a specific way, leading to shape morphing.[77] Magnetic poly(*N*-isopropyl acrylamide) hydrogel/elastomer hydrogel/elastomer hybrids could change shape and move in response to a direct or an alternating magnetic field. For example, Tang *et al.* designed a magnetic octopus-like hydrogel by stacking two different gels *via* 3D printing, where the magnetic nanoparticles incorporated acrylamide carbomer and the top part only contained acrylamide-carbomer ink (Fig. 5D).[84] The structure could be actuated using a programmed MF. Another approach is to apply a magnetic field to the dispensing nozzle of a 3D printer during the process of printing microparticles of neodymium–iron–boron (NdFeB) alloy and fumed silica nanoparticles in a silicone rubber matrix, leading to the reorientation of the ferromagnetic domains. Remote shape morphing can also be obtained by exploiting the magnetothermal effects of magnetic nanoparticles well dispersed in a gel network. In another report by Tang *et al.*, iron oxide nanoparticles were precipitated *in situ* on a pNIPAM hydrogel cross-linked with nanoclay, and a bilayer hydrogel was designed with the pNIPAM composite gel and an elastomer.[85] The bilayered gel underwent self-folding upon the application of an alternating MF due to the selective heating of the pNIPAM composite gel. *In situ* heating raised the local temperature of the gel higher than its LCST. Thus, the respective layer shrunk, causing a bend in the structure. However, the utility of MF-actuated hydrogel systems is limited due to the requirement of bulky instrumentation and potential interferences in medical imaging.

3.5. Other(s)

There are a few other actuating mechanisms for shape-morphing hydrogels. For example, pH-responsive hydrogels are comprised of ionic (cationic or anionic) pendant groups in their polymeric backbones.[29] Upon exposure to the desired pH and ionic strength solution, the pendant groups tend to ionize and form fixed charges on the polymer network, leading to swelling or shrinkage of the gel.[86] For instance, Gupta *et al.* reported the swelling of anionic hydrogels such as polyacrylic acid at a pH value higher than its pK_a (acid dissociation constants), owing to the ionization of the pendant groups and large osmotic swelling force.[87] Alternatively, the polyacrylamide-based cationic hydrogel shrunk at a pH value higher than its pK_a.[88] An electric field is an efficient way of driving shape morphing in hydrogels. Hydrogels immersed in an electrolyte solution generate charged ions and counter ions at a particular voltage, which are attracted to opposite directions by electrophoretic forces, leading to the electroosmotic movement of water molecules. The electrically induced diffusion of water molecules from the gel led to swelling/shrinkage.[89] The extent of deformation depended on the intrinsic (*e.g.*, stiffness and charge density) and extrinsic (*e.g.*, ionic strength and applied voltage) properties of the gel.[90] Han *et al.* prepared an electroactive gel-based ink comprised of a monomer, *i.e.*, acrylic acid, and a cross-linker, *i.e.*, PEGDA, which was printed using projection microstereolithography.[91] The 3D printed structures were subjected to different electric fields and the ionic strength of the electrolyte (PBS in this case) to analyze their bending curvatures. A few reports utilized more than one stimulation strategy to achieve shape-morphism. For example, Li *et al.* demonstrated an interesting hydrogel-metal hybrid responsive to light and magnetic fields.[92] Biological stimuli, such as enzymatic degradation, can also be utilized as a stimulation mechanism to realize shape morphing in gels.[93]

4. Tissue engineering and drug delivery applications of dynamic 4D hydrogels

4.1. Tissue engineering

Tissue engineering emerged from the field of biomaterials and refers to the application of an assembly of constructs of cells, scaffolds, and bioactive molecules to repair damaged tissues and restore cellular functionalities.[94,95] However, it is associated with four major challenges including material choice, cell source, limited vascularization, and poor drug delivery systems.[96] Consequently, shape-morphing hydrogels have emerged as alternative biomaterials possessing multiple, smart, and stimuli-responsive features.[23] Shape-morphing hydrogels exhibit a matching tissue stiffness and can mimic anisotropic tissue composition, allowing them to transform into predetermined shapes in response to external stimuli.[61] Hydrogel-based scaffolds can direct or induce cells to mature into a structure through a hierarchical differentiation process, resulting in replica tissue. The scaffold is essential for physical and structural support and promotes cell growth and optimum nutrient diffusion.[97] Conventional 3D printing technology failed to create tissue-mimicking dynamic matrices.[98–100] Therefore, developing 4D fabrication techniques is the key to creating a biological constructs that can substitute a defective tissue and restore organ function by fusing engineering principles with biological sciences.

This dynamic nature of tissue constructs printed with cells allows the assembly and disassembly of the printed parts. Cell-laden structures mature through self-regulation, migration, and matrix deposition, gradually developing into an active construct.[101] For instance, Garcia *et al.* co-polymerized acrylic acid with PEGMA to yield a pH-sensitive construct using SLA printing.[102] The resultant antimicrobial scaffolds demonstrated improved mammalian cell proliferation after curing with ethanol. In another report, Miao *et al.* prepared a temperature-responsive shape-shifting soybean oil-epoxidized acrylate-based scaffold.[103] The dynamic gels were biocompatible and endowed a proliferation support matrix for multipotent human bone marrow mesenchymal stem cells. Constante *et al.* developed a dual-component alginate-methylcellulose (extrusion printing) and PCL fiber (melt-electrowetting)-based scaffold that self-rolled in the presence of Ca^{2+} ions.[104] They reported that the C2C12 myoblasts grown on these 4D gel matrices showed good vitality, proliferation, and sequence positioning across the PCL fibers. Gladman *et al.* used an *N*,*N*-dimethyl acrylamide hydrogel to control the hardness and water solubility of the printed constructs.[61] The local orientation of the colloidal fibers followed a theoretical model for a three-dimensional structure, opening the door for multiple tissue engineering approaches. More interestingly, the hydrogel constructs printed with mammalian cells also demonstrated shape-deformation (Table 1). Recently, our group developed a bio-ink comprised of GelMA and PEGDM 8000 that could be fabricated with DLP printing with a visible range light source (405 nm). These printed hydrogels folded in response to water, were non-toxic, and showed continuous proliferation of embedded cells.[49] Below, we discuss numerous dynamic hydrogels and their importance in drug delivery and tissue regeneration (cardiac and neural tissue).

4.1.1. Cardiac tissue regeneration. Atherosclerosis and heart failure after myocardial infarction are among the most typical cardiovascular diseases and remains the primary contributor to morbidity and mortality.[116] Developing an operational equivalent for cardiac tissue restoration has spurred cardiovascular tissue engineering.[117] The dynamic cardiac structures may seamlessly integrate as they experience a curved architecture at the target site of the heart. Developing vascular stents with complex geometries can be difficult and time-consuming using traditional manufacturing techniques.[118,119] In this case, the combination of finite element analysis with 3D printing to make shape-morphing structures enables the study and preparation of various grafts. The physiological and anatomical characteristics of blood vessels, for instance, their complicated structural connections, indicate the need for 4D

Table 1 Summary of emerging 4D hydrogels for tissue engineering and drug delivery applications

Material	Fabrication strategy	Stimuli	Application	Characteristic feature	Ref.
Alginate and hyaluronic acid	Extrusion	Moisture	Vascular tissue	• Employs two biopolymers • Fabrication of hollow self-folding tubes • The diameter of the folded tube is ~20 μm • Enabled 4D bio fabrication (bone marrow cells)	67
Poly(glycerol dodecanoate) acrylate (PEGDA)	Extrusion	Temperature	Vascular stent	• Ideal for room temperature shape programming • Potential for deployment within the human body • Suitable thermo-rheological properties enabled the printing of multifunctional 3D structures	105
Soybean oil epoxidized acrylate (SOEA)	Photolithographic-stereolithographic-tandem strategy	Temperature	Cardiac tissue	• Rapid development of films (within seconds) having varied thicknesses • Printed constructs indicated unique surficial micropatterns • Biocompatible and promotes hMSC proliferation	106
GelMA and PEGDA	SLA	Solvent	Cardiac tissue	• A 4D cardiac patch with physiological adaptability • Designed to improve biomechanical properties and the dynamic integration of the patch with the beating heart • Increased cell engraftment and vascular supply in a murine chronic MI model	107
PEGDA, bisphenol A diglycidyl ether, poly(propylene glycol) bis (2-aminopropyl) ether, and decylamine	DLP and replica molding	Light	Cardiac tissue	• Cardiac construct with highly aligned microstructure and adjustable curvature • Capacity to actuate remote-controlled spatiotemporal transformation • Efficient method for manufacturing curved tissue architectures	108
Bisphenol A diglycidyl ether, decylamine, and poly (propylene glycol) bis(2-aminopropyl) ether, graphene nanoplatelets	FDM, extrusion, and replica molding	Temperature and light	Neural tissue	• Nanomaterial-engineered stimuli-responsive hydrogel • Dynamic and on-demand shape transformation • Created 3D patterned biological structures that can spatiotemporally control their shapes	109
SOEA	SLA	Solvent (water/ethanol)	Neural tissue	• Stress-induced shape transformation • A proof-of-concept of smart nerve guidance nano-engineered conduit • Created multi-responsive smart architectures	110
4-Hydroxy butyl acrylate, urethane-polyethylene glycol-polypropylene glycol (PU-EO-PO) monomer and fracture	DLP	Magnetoelectric	Neural tissue	• Developed electro-magnetized carbon nanocookies • Fostered neuron cell differentiation and proliferation *in vitro* and *in vivo* • Enhances cell adhesion and allows direct manipulation of electromagnetic stimulation of the cells • Showed magnetic field-guided *in vivo* neuron regeneration	111

Table 1 *(Contd.)*

Material	Fabrication strategy	Stimuli	Application	Characteristic feature	Ref.
Polyvinyl alcohol (PVA)	FDM	Moisture and temperature	Drug delivery (Allopurinol)	• Shapes were designed in principle to enable gastric retention • Temporary shapes were compatible with oral administration into capsules • Prototypes caused water-induced shape recovery	112
PEGDA	DLP and Projection micro stereolithography	Hydration/ dehydration	Drug delivery (Rhodamine B)	• Development of minimally invasive, pain-free, and easy-to-use microneedle • Bioinspired backward-facing curved barbs for enhanced tissue adhesion (>18-fold) • Sustained drug release	113
PVA and glycerol	Hot melt extrusion and FDM	Moisture	Drug delivery (Caffeine)	• Shape transformation at body temperature • Device could be administered *via* a catheter in a deformed state	114
Sodium alginate and Pluronic F127 diacrylate macromer	Extrusion	Ions	Drug delivery (Methotrexate)	• Dual network structure • A stable network is a cross-linked and reversible network that undergoes ionic cross-linking • Rapid *in vitro* drug release	115

printing. Creating *in vitro* biomimetic blood arteries is now very accessible due to the continuous growth of sophisticated techniques. Self-folding polymers can sometimes create blood vessels, which can then be organized into multilayered tube-like structures encapsulated with various cell types.[120,121]

Several recent studies have reported a 4D fabrication strategy to produce these intricate designs,[122,170] also allowing the synthetic cardiovascular stent to be delivered and performed at the site in a minimally invasive manner. In most investigations, the shape-morphing feature is attempted to be achieved under physiological conditions. In this regard, Cui *et al.* developed an innovative 4D cardiac patch using GelMA and PEGDA *via* beam-scanning SLA.[107] Light-mediated cross-linking created graded internal stress, resulting in shape-morphism to yield a wavy and curved structure. This biomimetic patch was cultured with induced pluripotent stem cells, mesenchymal stem cells, and cardiomyocyte maturation and vascularization were observed (Fig. 6A).[107] Three weeks after implantation, the patches developed a strong bond with the epicardium, improving vascular infiltration and cell engraftment and leading to cardiac regeneration. An implantable device that can be readily regulated at room temperature would be beneficial. Toward this, PGDA-based polymers that can inevitably adapt to the physiologically relevant environment and the structural and mechanical adaptability of biomedical implants led to the development of new regenerative therapies for cardiovascular disorders. These are useful methods for addressing issues and enhancing the endurance of the infarcted area.[123,124] To adhere to the heart and heal damaged myocardial tissue, the prepared scaffold patches should possess a curvature design that can create medically realistic surfaces for better alignment and incorporate dynamic mechanical stimulation.[125]

The application of NIR light has increased due to its non-intrusiveness, higher penetration depth, and ability to regulate shape modification.[109,126] Wang *et al.* showed that printing inks combined with graphene nanoplatelets can be used to develop micropatterned structures for the restoration of heart function.[108] Due to NIR-based photothermal effects, the constructs displayed a change, towards a curvature, thus imitating the native architecture of the heart (Fig. 6B).[108] This highlights the potential for controlling the building shape remotely and even cell distribution alongside myocardial maturation.[127] Toward this, Miao *et al.* demonstrated that smart SOEA inks can create cardiac patches using an integrated SLA and photolithography process. The hMSCs grown on the patches formed a micro pattern, thereby controlling the alignment and differentiation of the cells.[106] Due to the continuous self-folding and regeneration of the4D scaffold, it was employed as a myogenic bioreactor. Similarly, blood arteries can be built using a 4D self-folding polymer that, when moistened, can transform into a tube-like configuration.[22] In this regard, Zhang *et al.* created 50–500 mm diameter microvascular tubules using methacrylated GelMA and hyaluronic acid that mimics microvasculature (Fig. 6C-a).[71] Animal testing revealed that these constructs do not block circulation, promote vascularization, and boost the blood supply (Fig. 6C-b).[128] The formation of 3D micro-scaled hollow tubules (MHTs) from a 2D-planar geometry in response to environmental cues was realized to mimic small vascularized models. For instance, extrusion-based bioprinting was employed to create bilayer MHTs of molten electro-writing polymer composites and photo cross-linkable hydrogels.[19] Similarly, Kirillova *et al.* fabricated 20-micron size tubes using alginate and hyaluronic acid, and this adaptable 4D bio-fabrication architecture enabled the production of structures with sizes similar to the finest vessels.[67] Cui *et al.*

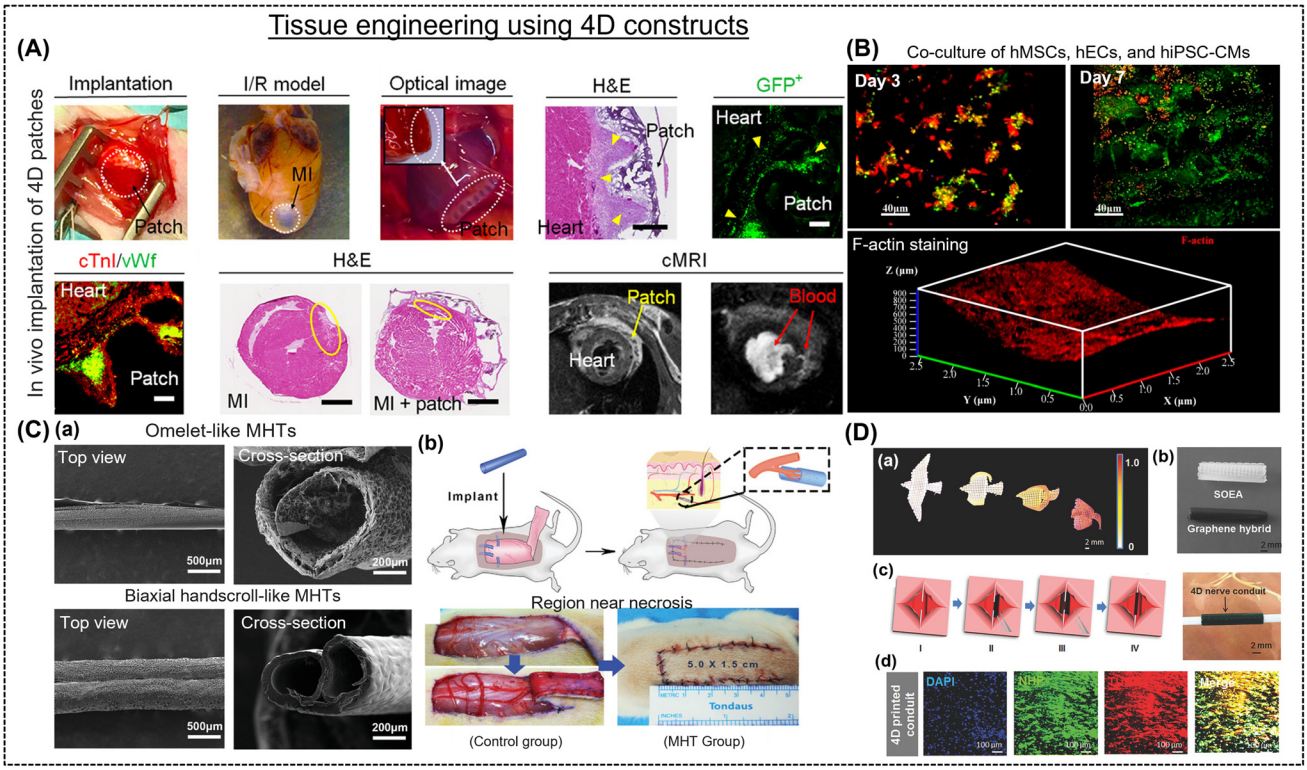

Fig. 6 (A) Implantation and long-term evaluation of 4D patches in a mouse model. Reproduced with permission.[107] Copyright 2020, Science. (B) Immunofluorescence staining images of a co-culture (hMSCs, hECs, and hiPSC-CMs) on biomimetic 4D cardiac tissue. F-actin staining of cells on the deformed shape. Reproduced with permission.[108,128] Copyright 2021, ACS. (C-a) SEM images of the "omelet"- and "biaxial handscroll"-like micro-scaled hollow tubules (MHTs). (C-b) Schematic representation of the MHTs surgically implanted beneath the skin flap. The left and right images in (C-b) are after the placement of GelMA MHTs and the suture of the random flap after surgery. Reproduced with permission.[128] Copyright 2020, Wiley Online Library. (D-a) Bird flying architectures designed with varying graphene concentrations (0–0.8%). (D-b) Dynamic nerve conduit prepared without graphene (white) and with 0.8% graphene (0.8 × 1.5 cm). (D-c) Representation of the tubulation of nerve conduit *via* a "thermo-mechanical programming" shape transformation. (D-d) Immunofluorescent images of neurogenic differentiation of hMSCs on the nerve conduit and its UV-crosslinked counterpart. Reproduced with permission.[110] Copyright 2018, Wiley Online Library.

enabled the development of micropatterned constructs using inkjet printing to precisely control the cell–cell arrangement. These structures exhibited distinct swelling rates (the top layer swelled slowly compared to the bottom), forming a curved construct on exposure to water. The sacrificial layer allowed the control of the initiation of the self-folding process of the hydrogel and facilitated easy culturing of HUVECs, thereby mimicking human microvessels.[129]

4.1.2. Neural tissue regeneration. The regeneration of traumatic injury or neurological disease-induced nerve defects is an extremely challenging clinical problem.[130–132] Neurons are formed during embryonic development but cannot regrow when they encounter damage in the nervous system. Axon regeneration is regulated by several intracellular processes, including cytoskeleton changes, nutrient transport, molecular trafficking, signaling, and epigenetic alterations.[133] Patients with neurological impairments only have a limited number of therapeutic options, and scientists and physicians continue to encounter formidable obstacles. Tissue engineering approaches have arisen from certain novel therapeutic approaches for treating neurodegenerative illnesses, and the unique attributes of 4D-printing technology, such as adaptive self-enturbulation and flawless integration, make them suitable substrates for neural tissue engineering.[130,134,171] Toward this, our group developed a dual-component hydrogel system, which served as a nerve-guiding conduit and repaired sciatic nerve defects in a rat model.[21] Miao *et al.* fabricated a programmable nerve-guiding conduit of SOEA and graphene to offer a minimally invasive operating procedure with dynamic activation that guides axonal regeneration and improves integration.[110] Graphene was used to modify the curvature and increase the conductivity of the conduit. At the same time, SOEA exhibited a structural metamorphosis (Fig. 6D).[110] The as-developed conduit showed a directed organization and increased expression for neurogenic differentiation with hMSCs. A thermo-sensitive PU-based hydrogel showed improved stiffness without incorporating any crosslinker.[135] Hsieh *et al.*[136] dispersed neural stem cells (NSCs) in a PU-based hydrogel before the incorporation of gelatin. The results indicated that printed bioproducts exhibited extraordinary proliferation and differentiation at the physiological temperature. The *in vivo* response of a biodegradable hydrogel in a zebrafish

model revealed that the 4D-printed products successfully rescued zebrafish from nerve injury. Similarly, Apsite *et al.*[137] developed nerve guide conduits (NGCs) using poly(glycerol sebacate) (PGS)-PCL/MA-HA-based bilayer mats. The results indicated that printed soft NGCs exhibited excellent biocompatibility and degradation resistance. Additionally, neuron cells (PC-12) cultured on artificial nerve grafts also displayed excellent cellular adhesion, differentiation, and proliferation. Wu *et al.*[138] also fabricated a self-healing hydrogel through 4D bioprinting, which could potentially be applied for nerve regeneration. In another report, Atoufi *et al.* displayed electric field-responsive agarose and alginate tetramer scaffolds possessing shape transformation properties to dispense anti-inflammatory drugs that heal nerve injuries, which efficiently supported the proliferation of pheochromocytoma cells.[139] Li *et al.* blended silk fibroin with polyacrylamide hydrogels that undergo *in situ* radical polymerization, enhancing peripheral nerve regeneration.[140] In another report, Hsiao *et al.* prepared a dual-stimuli (light and temperature) responsive acrylate-functionalized biodegradable polyurethane hydrogel.[141] This gel rapidly underwent thermal gelation at 37 °C, thus forming a compact structure, allowing for high-accuracy printing and accelerated neural differentiation. A unique composite approach was demonstrated by Liu *et al.* to construct tubular geometries using DIW employing a combination of thermoresponsive and non-thermoresponsive inks.[142] At 25 °C in water, these objects exhibited a variety of motions (including elongation, expansion, bending, and grasping) before resuming the native design at 50 °C. The horizontal or vertical placement directly influenced the movement type. These gel composites have great potential and can be used for nerve regeneration.

4.1.3. Bone and cartilage regeneration. Bone and cartilage tissue regeneration are complex processes that involve the coordinated action of multiple cellular and molecular pathways.[143,144] Bone regeneration typically begins with blood clot formation at the injured tissue site, followed by the accumulation of mesenchymal stem cells, which can differentiate into bone forming cells and further promote the proliferation and differentiation of cells to gradually remodel and mature bone tissue over time.[143] Alternatively, cartilage regeneration is a more challenging process due to its limited regenerative capacity. Injured cartilage tissue is typically replaced by scar tissue, which lacks the functional and structural properties of healthy cartilage.[144] Nevertheless, many strategies have been reported to induce cartilage regeneration, including the utilization of growth factors, tissue scaffolds, and cell-based therapies to stimulate proliferation and differentiation of chondrocytes. These specialized cells are often responsible for producing and maintaining cartilage matrix to heal the damaged tissue and restore its function. The soft and dynamic nature of 4D hydrogels is beneficial for soft tissue repair, while exhibiting limited potential toward hard tissue engineering such as bone. Therefore, here we will mainly highlight state-of-the-art 4D printing technology for cartilage engineering. Compared to conventional approaches, 4D hydrogels offer several advantages, for example cartilage is subject to variable mechanical loading, and these shape-shifting hydrogels can mimic the dynamic environment by adapting and responding to applied or produced mechanical stress or strain. In addition, 4D hydrogels enable precise spatial and temporal control of the biochemical and biomechanical cues to cells. This control is vital for guiding cell behavior and tissue repair in an organized and functional manner. For instance, Ding *et al.* demonstrated shape-morphing scaffold-free cell condensates with predetermined and intricate geometries.[145] They showed the fabrication of "C"- and helix-shaped robust 4D hydrogels mimicking cartilage-like tissues differentiated from human mesenchymal stem cells (Fig. 7A). The dynamic structures remained intact and stable for three weeks in chondrogenic media, which led to the generation of hydrogel-free 4D tissues. In another work, Alsberg's group prepared a jammed micro-flake hydrogel for the 4D bioprinting of cartilage-like tissue (Fig. 7B).[146] Interestingly, the shape changes in the hydrogels were also governed by varying the pH of the surrounding system at room temperature. Díaz-Payno *et al.* reported a dual-component smart multi-material system comprised of hyaluronan (high-swelling) and alginate (low-swelling) for cartilage engineering.[147] Both inks showed similar viscoelastic properties, sheer-thinning behaviors, and printing fidelity. The 4D phenomenon was observed due to their differential swelling *via* liquid immersion. The developed 4D gels demonstrated cell viability up to 28 days in chondrogenic medium and the curvature of the fabricated structures clearly presented a cartilage-like matrix, which was characterized by histology (Fig. 7C). The aforementioned 4D bioprinting systems enabled the fabrication of architecturally complex tissue constructs, while facilitating functional tissues. hMSCs are multipotent stem cells with the ability to differentiate into multiple connective tissue lineages in response to appropriate environmental cues, and thus may serve as a promising cell source for reconstructing tissues such as bone and cartilage.

4.2. Drug delivery systems

Drug delivery platforms have been designed to perform at their optimum range when paired with a particular application (such as maximizing drug efficacy, minimizing side effects, enhancing bioavailability, prolonging residence time, and reducing drug administration frequency).[148,149] The distribution method should be specifically tailored to the intended use and stimulus response to achieve optimal drug release outcomes. In this case, more advanced and target-specific systems can be made using the 4D printing approach. Advanced drug delivery devices can be created that allow programmed control of administered medicines, biomolecules, and cells. They can facilitate response-mediated, sustained administration and better retention at the targeted site.[150] Using 4D printing technology, tablets, dermal skin patches, nano-suspensions, and rectal and vaginal delivery systems can be created with excellent precision.[114,151,152] Combined, these factors will significantly lessen the efforts of medical staff, infection risk, operation, and patient recovery time.[112] Due to these character-

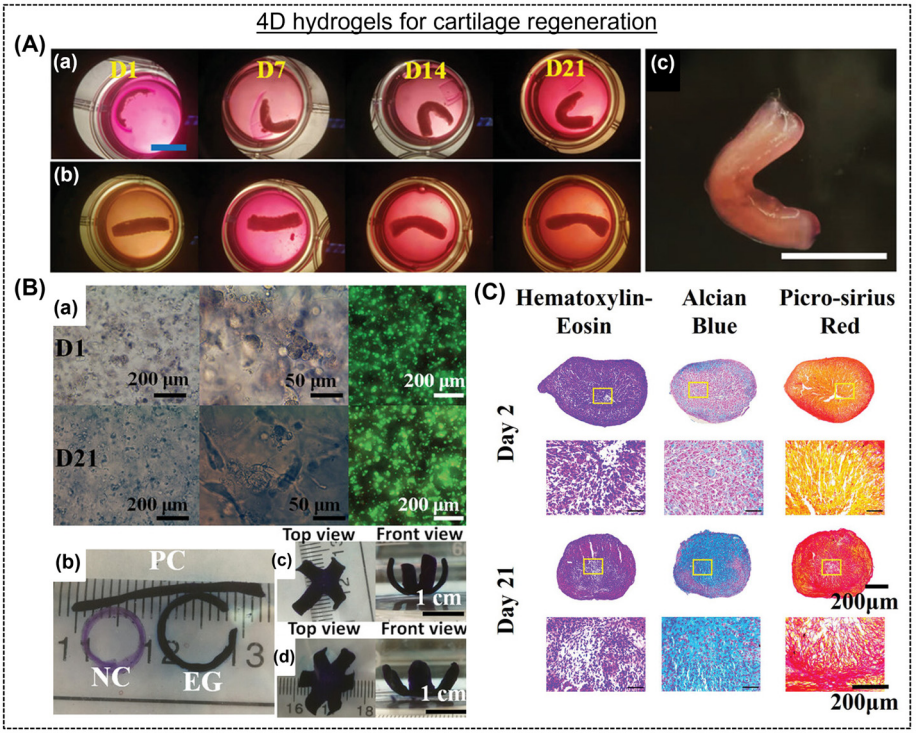

Fig. 7 (A) Changes in the shapes of human mesenchymal stem cell condensate-laden bilayer strip ((a) experimental and (b) control groups) grown in chondrogenic media at different times (day 1, 7, 14, and 21). A (c) "C"-shaped cartilage mimicking tissue after three weeks of culture. Scale bar is 10 mm. Reproduced with permission.[145] Copyright 2022, Wiley Online Library. (B) (a) Photomicrographs displaying morphology and distribution of cells together with live/dead staining assays after culturing in chondrogenic medium for day 1 and day 21. (B) (b) Printed hydrogels, (e) four- and (f) six-petal flower-shaped hydrogels after chondrogenesis for 21 days in culture medium. Reproduced with permission.[146] Copyright 2022, Wiley Online Library. (C) Histological analysis using hematoxylin and eosin (purple), Alcian blue, and picrosirius-red staining of MSC pellets cultured in chondrogenic conditions for different time interval.[147] Copyright 2022, Wiley Online Library.

istics, researchers can use a modified structure in response to an external stimulus for a dynamic function. Drug-hydrogel associations are necessary for efficient storage and release under controlled conditions. Numerous chemical and physical reactions have been investigated for their potential and efficient delivery.[153] For example, a UV-triggered chitosan-based helical micro-swimmer was fabricated by Bozuyuk *et al.*[154] The micro-swimmer showed good biodegradability and drug release. The core–shell hydrogel system in a 4D-printed capsule fabricated by Gupta *et al.*[155] released medications on demand at precise tissue site. The capsule contained ethylene glycol, poly(vinyl alcohol), and biomolecules in its core and gold nanorods (AuNRs) and poly(lactic-*co*-glycolic acid) in its shell. The photo-responsive AuNRs burst and released medicines upon to laser stimulation.

It is possible to create multiple organ-retentive devices meant to be kept inside organs and gradually release drugs in the interim. In this regard, Malachowski and colleagues fabricated a multi-fingered theragripper (TG) drug-eluting device using photolithography. It facilitated controlled drug release through its layers of pores, and as it entered the body, it spontaneously grabbed hold of the tissue. Consequently, it effectively immobilized at a specific place and delayed drug release, allowing for improved control and decreased adverse effects (Fig. 8A).[156] Recently, Zu and colleagues created a capsule using extrusion printing with an exterior made of a hydrogel (Fig. 8B).[157] This temperature-sensitive capsule could compress and release most of its contents within 48 h. The amount of MMP-2 increased in a tumor metastatic area, breaking down the collagen proteins in the tissue remodeling process and acting as a biological catalyst that causes the targeted release of anti-inflammatory medicines from negatively charged hydrogels. In this process, enzymes break down the drug-loaded hydrogel to distribute the medications to the appropriate bodily locations as needed.[158] In another report, Ceylan *et al.* developed a GelMA-based microrobot hydrogel that releases drugs by sensing MMP-2 in the microenvironment (Fig. 8C).[159] Consequently, the increase in the concentration of these proteases acts as a stimulus for drug release. Similarly, Li *et al.* prepared a hybrid-actuated soft microrobot with iron oxide particles, PHEMA, and PEGDA, which allowed the targeted delivery of anti-tumor medicines (Fig. 8D).[160] The therapeutic drug molecules used in 4D-printed devices are released after exposure to the appropriate stimulation from the designated sites. Osmolarity gradients can release the pertinent drug molecules from complicated multisome system frameworks.[161] For example, Wang and colleagues created alginate and diacrylate Pluronic-based 4D-printed drug delivery patches

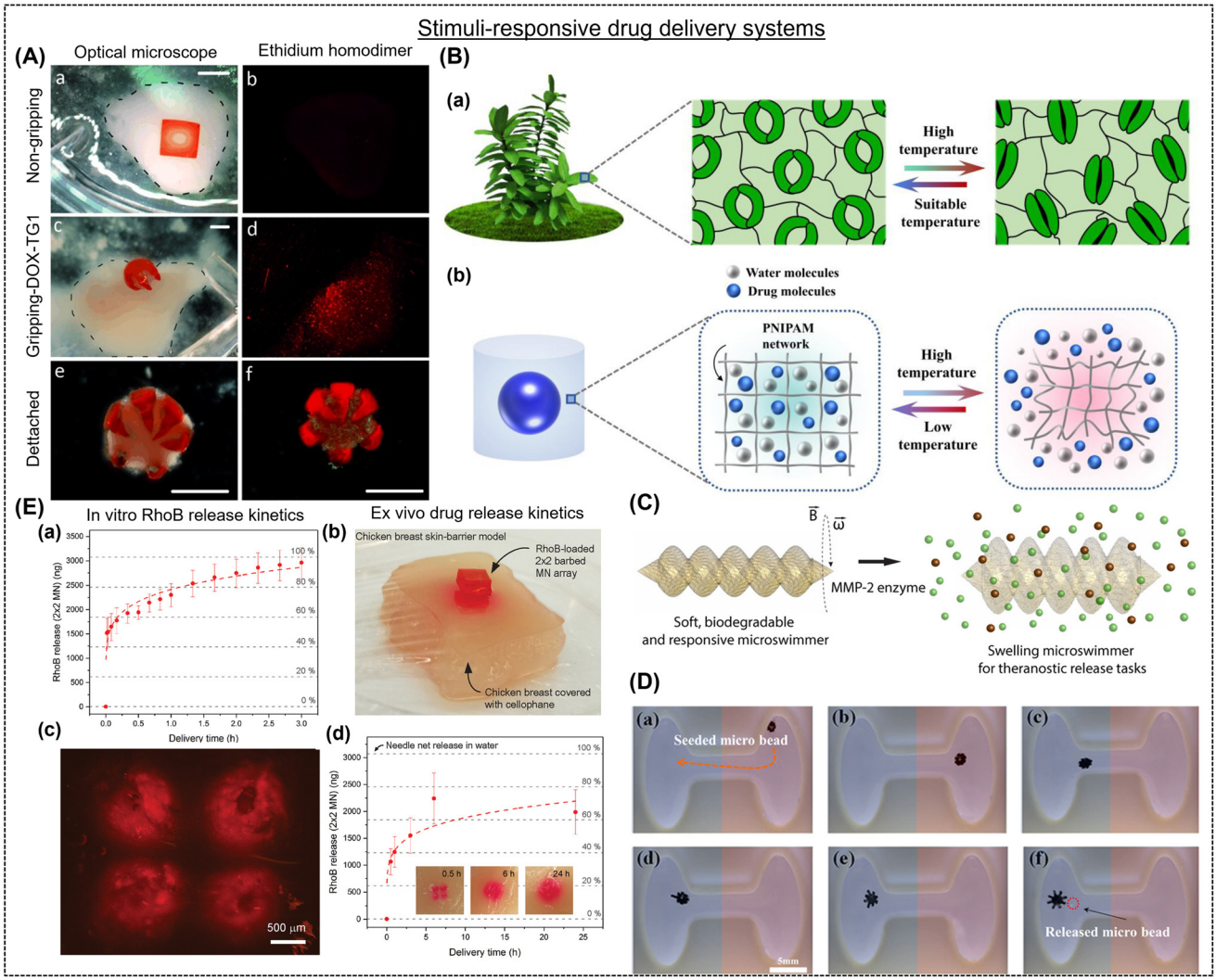

Fig. 8 (A) *In vitro* model of doxorubicin (DOX) elution from (a and b) non-gripping (negative control) and (c–e) theragripper ((b and c) attached and (c and d) detached). The scale bar in (A) is 2 mm. Reproduced with permission.[156] Copyright 2014, Wiley Online Library. (B-a) Schematic representation of opening and closing in response to temperature. (B-b) Dynamic water and drug transport channels in the hydrogel capsule microstructures. Reproduced with permission.[157] Copyright 2022, Elsevier. (C) Enzymatic drug delivery using a 3D-printed microswimmer (length = 20 μm and diameter = 6 μm) prepared by two-photon polymerization. Reproduced with permission.[159] Copyright 2019, ACS. (D) Magnetic field-actuated pH-responsive behavior of hydrogel-based soft microrobot. The red and blue areas represent high and low pH values, respectively. The scale bar in (D) is 5.0 mm. Reproduced with permission.[160] Copyright 2016, IOP Science. (E) (a) *In vitro* and (b) *ex vivo* drug release test using barbed microneedle array. (E-c) Fluorescence microscope image of a chicken breast skin-barrier model stained with RhoB-loaded microneedle array (0.5 h after insertion). (E-d) Quantification of released RhoB from microneedle array into the chicken breast at different intervals (0.5, 1, 3, 6, and 24 h). Reproduced with permission.[113] Copyright 2020, IOP Science.

and $CaCl_2$ was used to initiate the brief shape change under external stress, and the ionically cross-linked (reversible) network was recovered using a sodium carbonate solution.[115] The authors highlighted the effects of drug release based on the device shape and surface area. Conversely, Zhao *et al.* printed heparin-loaded bilayered GelMA hydrogels that fold into a tubular fashion in response to water and release about 70% of the drug over 30 h.[162] In another report, Melocchi *et al.* used FDM printing to create a temporary rod-shaped poly(vinyl alcohol) construct for easy insertion into the bladder.[114] After that, the hydrogels swelled to a curled shape as they came in contact with water for organ retention and rapidly released all the loaded molecules in 2 h. The same group focused their research in the area of extendable devices for retention in the stomach. The apparatus was anticipated to revert to its initial form as it encountered gastric fluids.[112] Han *et al.* constructed a PEGDA-based hypodermic needle array with curved barbs facing backward to improve tissue adherence while delivering drugs (Fig. 8E).[113] The photocurable polymer used in the original structures featured a gradient of cross-linking density, meaning that the tops of the barbs displayed more cross-linking than the bottoms. The barbs were oriented horizon-

tally. When the spikes dried, they curved backward to form a hook-like shape.

5. Feasibility of next-generation 4D hydrogels

Although 4D hydrogels show immense potential for biomedical applications, their journey towards widespread clinical use is associated with considerations regarding sustainability, safety, and efficient translation. Sustainability concerns arise from the materials and fabrication processes involved. Traditional hydrogel components such as synthetic polymers often possess poor biodegradability or require energy-intensive synthesis. Moving towards biocompatibility, naturally derived materials such as biopolymers or decellularized matrices offer a more sustainable alternative.[163] Fabrication techniques such as 3D/4D printing, while enabling precise control, can be limited by the use of solvents, high energy consumption and high costs, making them a poor choice for large-scale production. Thus, it is inevitable to explore biocompatible inks and optimize the printing parameters for sustainable practices.[164] Safety considerations stem from the potential cytotoxicity of the components, degradation products, or leachable unreacted chemicals of hydrogels. Rigorous *in vitro* and *in vivo* testing, together with biocompatibility assessments, are essential before clinical implementation.[165] Additionally, the dynamic nature of 4D hydrogels necessitates careful evaluation of potential unintended responses or immunogenic reactions triggered by their time-dependent transformations.

Clinical translation presents its own set of challenges. Scaling up production for clinical needs, while maintaining intricate design features and functionalities remains an ongoing hurdle. Conventional manufacturing techniques may not be readily adaptable, necessitating innovation in scalable fabrication methods. Furthermore, the inherent instability of some 4D hydrogels, prone to swelling-induced structural collapse or premature degradation, necessitates strategies to enhance their robustness for long-term *in vivo* applications. The mechanically fragile nature of certain 4D hydrogels also raises concerns about their ability to withstand physiological stresses, and strategies to improve their mechanical strength are actively pursued.[165,166]

Finally, commercial viability and availability are important hurdles. The high cost of material development, specialized equipment, and stringent regulatory requirements can hinder widespread adoption. Collaborative efforts among academia, industry, and regulatory bodies are crucial to bridge this gap and make 4D hydrogels more commercially accessible.[167] Although 4D hydrogels show immense promise for revolutionizing biomedicine, achieving their sustainable and safe clinical translation necessitates addressing sustainability concerns, ensuring rigorous safety evaluations, developing scalable fabrication methods, enhancing their stability and mechanical strength, and fostering collaborations to improve their commercial viability. Overcoming these challenges will pave the way for 4D hydrogels to realize their full potential in advancing human healthcare.

6. Conclusions, challenges, and futuristic vision

Shape morphism is a bioinspired event critical for the survival of living organisms to adapt to ever-changing, complex environments. Now, efforts are being directed toward developing synthetic materials capable of mimicking the behaviors that nature has perfected over centuries. Hydrogels have emerged as one of the most promising candidates among the shape-morphing materials. Shape deformations in hydrogels are observed due to the non-uniform distribution of internal stresses resulting from the asymmetrical swelling/shrinking of different parts of the same hydrogel system. These out-of-plane and in-plane gradients are created due to the differences in the local swelling behavior, amplifying the internal stresses under external stimuli. Actuators, including moisture, light, temperature, pH, and magnetic field, and their role in achieving the desired and pre-determined shape were presented. Herein, we discussed the various 4D fabrication techniques (extrusion printing, light-based 3D printing, and solvent casting) to prepare shape-shifting hydrogels. Differences between mono- and dual-component hydrogel systems, the capabilities of 3D constructs to undergo uni- or bi-directional shape changes, and advantages of composite hydrogels compared to their pristine counterparts were meticulously discussed. These 4D gels have shown remarkable potential as dynamic tissue scaffolds for regenerative engineering and drug-delivery applications due to their shape-morphing properties. This review also highlighted the advantages of 4D printing over the conventional 3D printing to develop live tissue scaffolds with intricate designs.

The development of shape-morphing hydrogels involves critical consideration of many factors, such as material choice, stimuli responsiveness, and fabrication process, to achieve predetermined complex shapes and precise control of the shape-change kinetics and reversibility. A mechanistic understanding of the material behavior and its response to external stimuli is crucial. In this regard, theoretical insights using tools such as finite element analysis, molecular dynamics, density functional theory, and other bimolecular simulations can enable the prediction of cell–material interaction to provide advanced architectures. Significant attention should be provided to increase the magnitude of shape change and larger out-of-plane movements by carefully selecting biopolymers and designing 3D constructs. The hydrogel recipe must incorporate multi-stimuli responsive moieties to achieve multi-step shape transformations and complicated designs. Triggers such as temperature and magnetic field should be active in the physiological range to be exploited to their fullest potential. This information is useful for guidance in designing effective and

tailored materials for tissue-specific applications. Additionally, pre-clinical investigations should be conducted to assess the safety, strength, and efficacy of these shape-morphing hydrogels to repair damaged tissue. The hydrogel matrix must be able to change shape *in situ* and promote cell adherence and proliferation for efficient regeneration. The positioning of hydrogels is challenging due to body fluids, making them bend/fold/twist before reaching the target site.[168] These critical issues must be resolved for the successful translation of shape-morphing biomaterials.

The development of shape-morphing hydrogels through additive manufacturing, including DIW and DLP, has been presented over the years to achieve precise, programmable, and customizable designs. Unlike solvent casting, which is a natural air-drying process, 3D printing technology enables the development of multi-material-based scaffolds with intricate patterns, offering the possibility of integrating piezoelectric biopolymers and sensors to potentially develop state-of-the-art bioelectronics interfaces. Adopting this idea will enable harvesting mechanical energy from motions such as bending, twisting, and rolling during shape transformations to develop self-powered biodevices. Data science has emerged as a dominant research theme in several engineering disciplines in the past decade. The application of deep-learning algorithms and artificial intelligence in shape-morphing hydrogels can help predict the tissue response by varying the biopolymers, composition, size, and arrangement of stimuli-response and non-responsive layers in hydrogel systems. Further integrating hydrogels with Internet of Things (IoT) technology will enable real-time monitoring of *in situ* shape transformations, regenerative processes, and surrounding organs. In summary, the futuristic growth in shape-morphing hydrogels needs immense collaboration among biomedical engineers, biomaterial scientists, data scientists, and clinicians. Reliable, quantitative, and rapid tools must be developed for advanced mechanistic insights into the correlation between shape-morphing hydrogels and tissue regeneration. Intelligent biomaterials and the predictive capabilities of data science will profoundly accelerate the discovery of next-generation hydrogel-assisted regenerative therapy.

Conflicts of interest

The authors declare no conflict of interest.

Acknowledgements

This work was supported by the Department of Science and Technology (DST) sponsored Innovation in Science Pursuit for Inspired Research (INSPIRE) Faculty Programme (DST/INSPIRE/04/2021/001535). The authors acknowledge support from the Science and Engineering Research Board (SERB), Government of India (IPA/2020/000025).

References

1 S.-J. Jeon, A. W. Hauser and R. C. Hayward, *Acc. Chem. Res.*, 2017, **50**, 161–169.
2 H. Le Ferrand, K. S. Riley and A. F. Arrieta, *Bioinspiration Biomimetics*, 2022, **17**, 046002.
3 Z. J. Wang, W. Hong, Z. L. Wu and Q. Zheng, *Angew. Chem., Int. Ed.*, 2017, **56**, 15974–15978.
4 H. Kim, S. Ahn, D. M. Mackie, J. Kwon, S. H. Kim, C. Choi, Y. H. Moon, H. B. Lee and S. H. Ko, *Mater. Today*, 2020, **41**, 243–269.
5 R. S. Kularatne, H. Kim, M. Ammanamanchi, H. N. Hayenga and T. H. Ware, *Chem. Mater.*, 2016, **28**, 8489–8492.
6 D. Jiao, Q. L. Zhu, C. Y. Li, Q. Zheng and Z. L. Wu, *Acc. Chem. Res.*, 2022, **55**, 1533–1545.
7 R. V. Ulijn, N. Bibi, V. Jayawarna, P. D. Thornton, S. J. Todd, R. J. Mart, A. M. Smith and J. E. Gough, *Mater. Today*, 2007, **10**, 40–48.
8 J. M. Rosiak and F. Yoshii, *Nucl. Instrum. Methods Phys. Res., Sect. B*, 1999, **151**, 56–64.
9 A. S. Hoffman, *Adv. Drug Delivery Rev.*, 2012, **64**, 18–23.
10 A. Joshi, S. Choudhury, S. B. Gugulothu, S. S. Visweswariah and K. Chatterjee, *Biomacromolecules*, 2022, **23**, 2730–2751.
11 Z. U. Arif, M. Y. Khalid, R. Noroozi, A. Sadeghianmaryan, M. Jalalvand and M. Hossain, *Int. J. Biol. Macromol.*, 2022, **218**, 930–968.
12 E. M. White, J. Yatvin, J. B. Grubbs, J. A. Bilbrey and J. Locklin, *J. Polym. Sci., Part B: Polym. Phys.*, 2013, **51**, 1084–1099.
13 Z. U. Arif, M. Y. Khalid, W. Ahmed and H. Arshad, *Bioprinting*, 2022, **27**, e00203.
14 X. He, Y. Sun, J. Wu, Y. Wang, F. Chen, P. Fan, M. Zhong, S. Xiao, D. Zhang, J. Yang and J. Zheng, *J. Mater. Chem. C*, 2019, **7**, 4970–4980.
15 D. Tan, A. Nokhodchi and M. Maniruzzaman, *3D and 4D Printing in Biomedical Applications*, Wiley, 2019, pp. 25–52.
16 Z. Jiang, B. Diggle, M. L. Tan, J. Viktorova, C. W. Bennett and L. A. Connal, *Adv. Sci.*, 2020, **7**, 17.
17 H. Kadry, S. Wadnap, C. Xu and F. Ahsan, *Eur. J. Pharm. Sci.*, 2019, **135**, 60–67.
18 N. Shahrubudin, T. C. Lee and R. Ramlan, *Procedia Manuf.*, 2019, **35**, 1286–1296.
19 K. J. De France, F. Xu and T. Hoare, *Adv. Healthcare Mater.*, 2017, **7**, 1.
20 M. V. Risbud, A. A. Hardikar, S. V. Bhat and R. R. Bhonde, *J. Controlled Release*, 2000, **68**, 23–30.
21 A. Joshi, S. Choudhury, V. S. Baghel, S. Ghosh, S. Gupta, D. Lahiri, G. K. Ananthasuresh and K. Chatterjee, *Adv. Healthcare Mater.*, 2023, **12**, 24.
22 D. K. Patel, A. H. Sakhaei, M. Layani, B. Zhang, Q. Ge and S. Magdassi, *Adv. Mater.*, 2017, **29**, 1606000.
23 S. S. Imam, A. Hussain, M. A. Altamimi and S. Alshehri, *Polymers*, 2021, **13**, 3858.

24 A. Rath and P. Theato, *Adv. Funct. Mater.*, 2019, **30**, 1902959.
25 D. Yang, J. Xiao, B. Wang, L. Li, X. Kong and J. Liao, *Mater. Sci. Eng., C*, 2019, **104**, 109927.
26 N. Asadi, A. Mehdipour, M. Ghorbani, M. Mesgari-Abbasi, A. Akbarzadeh and S. Davaran, *Int. J. Biol. Macromol.*, 2021, **193**, 734–747.
27 A. Kirillova and L. Ionov, *J. Mater. Chem. B*, 2019, **7**, 1597–1624.
28 M. N. I. Shiblee, K. Ahmed, M. Kawakami and H. Furukawa, *Adv. Mater. Technol.*, 2019, **4**, 1–10.
29 X. Liu, M. Gao, J. Chen, S. Guo, W. Zhu, L. Bai, W. Zhai, H. Du, H. Wu, C. Yan, Y. Shi, J. Gu, H. J. Qi and K. Zhou, *Adv. Funct. Mater.*, 2022, **32**, 2203323.
30 Y. Dong, S. Wang, Y. Ke, L. Ding, X. Zeng, S. Magdassi and Y. Long, *Adv. Mater. Technol.*, 2020, **5**, 1–19.
31 M. Champeau, D. A. Heinze, T. N. Viana, E. R. de Souza, A. C. Chinellato and S. Titotto, *Adv. Funct. Mater.*, 2020, **30**, 1–22.
32 S. Roy Barman, P. Gavit, S. Chowdhury, K. Chatterjee and A. Nain, *JACS Au*, 2023, **3**, 2930–2947.
33 Y. Wang, R. K. Kankala, C. Ou, A. Chen and Z. Yang, *Bioact. Mater.*, 2022, **9**, 198–220.
34 Q. Zhao, J. Wang, H. Cui, H. Chen, Y. Wang and X. Du, *Adv. Funct. Mater.*, 2018, **28**, 1801027.
35 S. Mura, J. Nicolas and P. Couvreur, *Nat. Mater.*, 2013, **12**, 991–1003.
36 H. Hu, C. Huang, M. Galluzzi, Q. Ye, R. Xiao, X. Yu and X. Du, *Research*, 2021, **1–12**, 9786128.
37 U. Fasel, D. Keidel, L. Baumann, G. Cavolina, M. Eichenhofer and P. Ermanni, *Manuf. Lett.*, 2020, **23**, 85–88.
38 M. Zarek, N. Mansour, S. Shapira and D. Cohn, *Macromol. Rapid Commun.*, 2016, **38**, 1600628.
39 H. Yi, D. Kim, Y. Kim, D. Kim, J. Koh and M.-J. Kim, *Autom. Constr.*, 2020, **114**, 103151.
40 L. Chen, M. Weng, F. Huang and W. Zhang, *Sens. Actuators, B*, 2019, **282**, 384–390.
41 A. P. Piedade, *J. Funct. Biomater.*, 2019, **10**, 9.
42 M. Mao, J. He, X. Li, B. Zhang, Q. Lei, Y. Liu and D. Li, *Micromachines*, 2017, **8**, 113.
43 A. Joshi, S. Choudhury, V. S. Baghel, S. Ghosh, S. Gupta, D. Lahiri, G. K. Ananthasuresh, and K. Chatterjee, *Adv. Healthcare Mater.*, 2023, **12**, e2300701.
44 Z. Mao, K. Zhu, L. Pan, G. Liu, T. Tang, Y. He, J. Huang, J. Hu, K. W. Y. Chan and J. Lu, *Adv. Mater. Technol.*, 2020, **5**, 1900974.
45 J. Lai, X. Ye, J. Liu, C. Wang, J. Li, X. Wang, M. Ma and M. Wang, *Mater. Des.*, 2021, **205**, 109699.
46 S. Parimita, A. Kumar, H. Krishnaswamy and P. Ghosh, *J. Manuf. Process.*, 2023, **85**, 875–884.
47 S. Naficy, R. Gately, R. Gorkin, H. Xin and G. M. Spinks, *Macromol. Mater. Eng.*, 2017, **302**, 1600212.
48 Z. Zhao, X. Kuang, C. Yuan, H. J. Qi and D. Fang, *ACS Appl. Mater. Interfaces*, 2018, **10**, 19932–19939.
49 S. B. Gugulothu and K. Chatterjee, *ACS Macro Lett.*, 2023, **12**, 494–502.
50 X. Kuang, J. Wu, K. Chen, Z. Zhao, Z. Ding, F. Hu, D. Fang and H. J. Qi, *Sci. Adv.*, 2019, **5**, 1–9.
51 D. J. Roach, X. Sun, X. Peng, F. Demoly, K. Zhou and H. J. Qi, *Adv. Funct. Mater.*, 2022, **32**, 2203236.
52 F. V. Borbolla-Jiménez, S. I. Peña-Corona, S. J. Farah, M. T. Jiménez-Valdés, E. Pineda-Pérez, A. Romero-Montero, M. L. Del Prado-Audelo, S. A. Bernal-Chávez, J. J. Magaña and G. Leyva-Gómez, *Pharmaceutics*, 2023, **15**, 1914.
53 S. R. Barman, S. W. Chan, F. C. Kao, H. Y. Ho, I. Khan, A. Pal, C. C. Huang and Z. H. Lin, *Sci. Adv.*, 2023, **9**, 1–15.
54 G. Guo, Q. Wu, F. Liu, J. Yin, Z. L. Wu, Q. Zheng and J. Qian, *Adv. Funct. Mater.*, 2021, **32**, 2108548.
55 Z. Xu and J. Fu, *ACS Appl. Mater. Interfaces*, 2020, **12**, 26476–26484.
56 R. Yu, L. Zhu, Y. Xia, J. Liu, J. Liang, J. Xu, B. Wang and S. Wang, *Adv. Mater. Interfaces*, 2022, **9**, 2200401.
57 A. Ding, O. Jeon, R. Tang, Y. Bin Lee, S. J. Lee and E. Alsberg, *Adv. Sci.*, 2021, **8**, 2004616.
58 A. Ding, S. J. Lee, S. Ayyagari, R. Tang, C. T. Huynh and E. Alsberg, *Bioact. Mater.*, 2022, **7**, 324–332.
59 L. Tang, L. Wang, X. Yang, Y. Feng, Y. Li and W. Feng, *Prog. Mater. Sci.*, 2021, **115**, 100702.
60 J. Cao, C. Zhou, G. Su, X. Zhang, T. Zhou, Z. Zhou and Y. Yang, *Adv. Mater.*, 2019, **31**, 1900042.
61 A. S. Gladman, E. A. Matsumoto, R. G. Nuzzo, L. Mahadevan and J. A. Lewis, *Nat. Mater.*, 2016, **15**, 413–418.
62 Z. Ji, C. Yan, B. Yu, X. Zhang, M. Cai, X. Jia, X. Wang and F. Zhou, *Adv. Mater. Technol.*, 2019, **4**, 1800713.
63 Y. Park and X. Chen, *J. Mater. Chem. A*, 2020, **8**, 15227–15244.
64 P. D. C. Costa, D. C. S. Costa, T. R. Correia, V. M. Gaspar and J. F. Mano, *Adv. Mater. Technol.*, 2021, **6**, 1–21.
65 K. Shariati, A. S. Ling, S. Fuchs, B. Dillenburger, W. Liu and M. Ma, *Adv. Funct. Mater.*, 2022, **32**, 1–45.
66 S. Tawfick, M. De Volder, D. Copic, S. J. Park, C. R. Oliver, E. S. Polsen, M. J. Roberts and A. J. Hart, *Adv. Mater.*, 2012, **24**, 1628–1674.
67 A. Kirillova, R. Maxson, G. Stoychev, C. T. Gomillion and L. Ionov, *Adv. Mater.*, 2017, **29**, 1703443.
68 V. P. Anju, R. Pratoori, D. K. Gupta, R. Joshi, R. K. Annabattula and P. Ghosh, *Soft Matter*, 2020, **16**, 4162–4172.
69 G. Pasparakis and C. Tsitsilianis, *Polymer*, 2020, **211**, 123146.
70 I. Bischofberger and V. Trappe, *Sci. Rep.*, 2015, **5**, 15520.
71 L. Zhang, Y. Xiang, H. Zhang, L. Cheng, X. Mao, N. An, L. Zhang, J. Zhou, L. Deng, Y. Zhang, X. Sun, H. A. Santos and W. Cui, *Adv. Sci.*, 2020, **7**, 1903553.
72 T. Manouras and M. Vamvakaki, *Polym. Chem.*, 2017, **8**, 74–96.
73 H. Kim, J. Kang, Y. Zhou, A. S. Kuenstler, Y. Kim, C. Chen, T. Emrick and R. C. Hayward, *Adv. Mater.*, 2019, **31**, 1900932.
74 M. Czugala, C. O'Connell, C. Blin, P. Fischer, K. J. Fraser, F. Benito-Lopez and D. Diamond, *Sens. Actuators, B*, 2014, **194**, 105–113.

75 Y. Luo, X. Lin, B. Chen and X. Wei, *Biofabrication*, 2019, **11**, 045019.
76 P. Xue, H. K. Bisoyi, Y. Chen, H. Zeng, J. Yang, X. Yang, P. Lv, X. Zhang, A. Priimagi, L. Wang, X. Xu and Q. Li, *Angew. Chem., Int. Ed.*, 2021, **60**, 3390–3396.
77 Z. J. Wang, C. Y. Li, X. Y. Zhao, Z. L. Wu and Q. Zheng, *J. Mater. Chem. B*, 2019, **7**, 1674–1678.
78 Y. H. Lai, S. Roy Barman, A. Ganguly, A. Pal, J. H. Yu, S. H. Chou, E. W. Huang, Z. H. Lin and S. Y. Chen, *Chem. Eng. J.*, 2023, **476**, 146744.
79 A. Chan, R. P. Orme, R. A. Fricker and P. Roach, *Adv. Drug Delivery Rev.*, 2013, **65**, 497–514.
80 J. K. Wychowaniec and D. F. Brougham, *Adv. Sci.*, 2022, **9**, 2202278.
81 X. Ni, X. Xing, Y. Deng and Z. Li, *Pharmaceutics*, 2023, **15**, 982.
82 A. Pardo, M. Gómez-Florit, S. Barbosa, P. Taboada, R. M. A. Domingues and M. E. Gomes, *ACS Nano*, 2021, **15**, 175–209.
83 Z. Liu, J. Liu, X. Cui, X. Wang, L. Zhang and P. Tang, *Front. Chem.*, 2020, **8**, 1–17.
84 J. Tang, Q. Yin, Y. Qiao and T. Wang, *ACS Appl. Mater. Interfaces*, 2019, **11**, 21194–21200.
85 J. Tang, Z. Tong, Y. Xia, M. Liu, Z. Lv, Y. Gao, T. Lu, S. Xie, Y. Pei, D. Fang and T. J. Wang, *J. Mater. Chem. B*, 2018, **6**, 2713–2722.
86 J. Fu, F. Yang and Z. Guo, *New J. Chem.*, 2018, **42**, 17162–17180.
87 P. Gupta, K. Vermani and S. Garg, *Drug Discovery Today*, 2002, **7**, 569–579.
88 P. Yuan, J. M. McCracken, D. E. Gross, P. V. Braun, J. S. Moore and R. G. Nuzzo, *Soft Matter*, 2017, **13**, 7312–7317.
89 T. Shiga and T. Kurauchi, *J. Appl. Polym. Sci.*, 1990, **39**, 2305–2320.
90 J. Lin, Q. Tang, D. Hu, X. Sun, Q. Li and J. Wu, *Colloids Surf., A*, 2009, **346**, 177–183.
91 D. Han, C. Farino, C. Yang, T. Scott, D. Browe, W. Choi, J. W. Freeman and H. Lee, *ACS Appl. Mater. Interfaces*, 2018, **10**, 17512–17518.
92 C. Li, G. C. Lau, H. Yuan, A. Aggarwal, V. L. Dominguez, S. Liu, H. Sai, L. C. Palmer, N. A. Sather, T. J. Pearson, D. E. Freedman, P. K. Amiri, M. O. de la Cruz and S. I. Stupp, *Sci. Robot.*, 2020, **5**, 1–12.
93 B. Narupai, P. T. Smith and A. Nelson, *Adv. Funct. Mater.*, 2021, **31**, 2011012.
94 B. Dhandayuthapani, Y. Yoshida, T. Maekawa and D. S. Kumar, *Int. J. Polym. Sci.*, 2011, **2011**, 1–19.
95 N. Nguyen, Z. H. Lin, S. R. Barman, C. Korupalli, J. Y. Cheng, N. X. Song, Y. Chang, F. L. Mi, H. L. Song, H. W. Sung and Y. J. Lin, *Nano Energy*, 2022, **99**, 107393.
96 H. Bramfeld, G. Sabra, V. Centis and P. Vermette, *Curr. Med. Chem.*, 2010, **17**, 3944–3967.
97 S. Chung and M. W. King, *Biotechnol. Appl. Biochem.*, 2011, **58**, 423–438.
98 J. Jang, H.-G. Yi and D.-W. Cho, *ACS Biomater. Sci. Eng.*, 2016, **2**, 1722–1731.
99 T. Li, J. Chang, Y. Zhu and C. Wu, *Adv. Healthcare Mater.*, 2020, **9**, 2000208.
100 A. Do, B. Khorsand, S. M. Geary and A. K. Salem, *Adv. Healthcare Mater.*, 2015, **4**, 1742–1762.
101 S. Ghosh, S. Chaudhuri, P. Roy and D. Lahiri, *Regener. Eng. Transl. Med.*, 2023, **9**, 339–365.
102 C. Garcia, A. Gallardo, D. López, C. Elvira, A. Azzahti, E. Lopez-Martinez, A. L. Cortajarena, C. M. González-Henríquez, M. A. Sarabia-Vallejos and J. Rodríguez-Hernández, *ACS Appl. Bio Mater.*, 2018, **1**, 1337–1347.
103 S. Miao, W. Zhu, N. J. Castro, M. Nowicki, X. Zhou, H. Cui, J. P. Fisher and L. G. Zhang, *Sci. Rep.*, 2016, **6**, 27226.
104 G. Constante, I. Apsite, H. Alkhamis, M. Dulle, M. Schwarzer, A. Caspari, A. Synytska, S. Salehi and L. Ionov, *ACS Appl. Mater. Interfaces*, 2021, **13**, 12767–12776.
105 C. Zhang, D. Cai, P. Liao, J.-W. Su, H. Deng, B. Vardhanabhuti, B. D. Ulery, S.-Y. Chen and J. Lin, *Acta Biomater.*, 2021, **122**, 101–110.
106 S. Miao, H. Cui, M. Nowicki, S. Lee, J. Almeida, X. Zhou, W. Zhu, X. Yao, F. Masood, M. W. Plesniak, M. Mohiuddin and L. G. Zhang, *Biofabrication*, 2018, **10**, 035007.
107 H. Cui, C. Liu, T. Esworthy, Y. Huang, Z. Yu, X. Zhou, H. San, S. Lee, S. Y. Hann, M. Boehm, M. Mohiuddin, J. P. Fisher and L. G. Zhang, *Sci. Adv.*, 2020, **6**, 1–12.
108 Y. Wang, H. Cui, Y. Wang, C. Xu, T. J. Esworthy, S. Y. Hann, M. Boehm, Y.-L. Shen, D. Mei and L. G. Zhang, *ACS Appl. Mater. Interfaces*, 2021, **13**, 12746–12758.
109 H. Cui, S. Miao, T. Esworthy, S. Lee, X. Zhou, S. Y. Hann, T. J. Webster, B. T. Harris and L. G. Zhang, *Nano Res.*, 2019, **12**, 1381–1388.
110 S. Miao, H. Cui, M. Nowicki, L. Xia, X. Zhou, S. Lee, W. Zhu, K. Sarkar, Z. Zhang and L. G. Zhang, *Adv. Biosyst.*, 2018, **2**, 1800101.
111 J.-H. Fang, H.-H. Hsu, R.-S. Hsu, C.-K. Peng, Y.-J. Lu, Y.-Y. Chen, S.-Y. Chen and S.-H. Hu, *NPG Asia Mater.*, 2020, **12**, 61.
112 A. Melocchi, M. Uboldi, N. Inverardi, F. Briatico-Vangosa, F. Baldi, S. Pandini, G. Scalet, F. Auricchio, M. Cerea, A. Foppoli, A. Maroni, L. Zema and A. Gazzaniga, *Int. J. Pharm.*, 2019, **571**, 118700.
113 D. Han, R. S. Morde, S. Mariani, A. A. La Mattina, E. Vignali, C. Yang, G. Barillaro and H. Lee, *Adv. Funct. Mater.*, 2020, **30**, 1909197.
114 A. Melocchi, N. Inverardi, M. Uboldi, F. Baldi, A. Maroni, S. Pandini, F. Briatico-Vangosa, L. Zema and A. Gazzaniga, *Int. J. Pharm.*, 2019, **559**, 299–311.
115 Y. Wang, Y. Miao, J. Zhang, J. P. Wu, T. B. Kirk, J. Xu, D. Ma and W. Xue, *Mater. Sci. Eng., C*, 2018, **84**, 44–51.
116 S. Xu, M. Bendeck and A. I. Gotlieb, *Cardiovascular Pathology*, Elsevier, 2016, pp. 85–124.

117 H. Cui, S. Miao, T. Esworthy, X. Zhou, S. Lee, C. Liu, Z. Yu, J. P. Fisher, M. Mohiuddin and L. G. Zhang, *Adv. Drug Delivery Rev.*, 2018, **132**, 252–269.
118 D. Xue, Y. Wang, J. Zhang, D. Mei, Y. Wang and S. Chen, *ACS Appl. Mater. Interfaces*, 2018, **10**, 19428–19435.
119 W. Hua, W. Shi, K. Mitchell, L. Raymond, R. Coulter, D. Zhao and Y. Jin, *Chinese J. Mech. Eng. Addit. Manuf. Front.*, 2022, **1**, 100020.
120 A. Bandyopadhyay, Y. Zhang and B. Onuike, *Virtual Phys. Prototyping*, 2022, **17**, 256–294.
121 D. G. Tamay, T. Dursun Usal, A. S. Alagoz, D. Yucel, N. Hasirci and V. Hasirci, *Front. Bioeng. Biotechnol.*, 2019, **7**, 1–22.
122 T. van Manen, S. Janbaz, K. M. B. Jansen and A. A. Zadpoor, *Commun. Mater.*, 2021, **2**, 56.
123 Z. Azhar, N. Haque, S. Ali, M. Mozafari and F. Sefat, in *Handbook of Tissue Engineering Scaffolds: Volume One*, Elsevier, 2019, pp. 705–728.
124 A. Khan, R. Joshi, M. K. Sharma, A. Ganguly, P. Parashar, T. W. Wang, S. Lee, F. C. Kao and Z. H. Lin, *Nano Energy*, 2024, **119**, 109051.
125 Y. Wang, H. Cui, T. Esworthy, D. Mei, Y. Wang and L. G. Zhang, *Adv. Mater.*, 2022, **34**, 2109198.
126 F. D. Jochum and P. Theato, *Chem. Soc. Rev.*, 2013, **42**, 7468–7483.
127 M. S. Spach, J. F. Heidlage, R. C. Barr and P. C. Dolber, *Heart Rhythm*, 2004, **1**, 500–515.
128 L. Zhang, Y. Xiang, H. Zhang, L. Cheng, X. Mao, N. An, L. Zhang, J. Zhou, L. Deng, Y. Zhang, X. Sun, H. A. Santos and W. Cui, *Adv. Sci.*, 2020, **7**, 1903553.
129 C. Cui, D.-O. Kim, M. Y. Pack, B. Han, L. Han, Y. Sun and L.-H. Han, *Biofabrication*, 2020, **12**, 045018.
130 O. A. Carballo-Molina and I. Velasco, *Front. Cell. Neurosci.*, 2015, **9**, 1–12.
131 A. R. Nectow, K. G. Marra and D. L. Kaplan, *Tissue Eng., Part B*, 2012, **18**, 40–50.
132 C. H. Fan, H. C. Tsai, Y. S. Tsai, H. C. Wang, Y. C. Lin, P. H. Chiang, N. Wu, M. H. Chou, Y. J. Ho, Z. H. Lin and C. K. Yeh, *ACS Nano*, 2023, **17**, 9140–9154.
133 M. Curcio and F. Bradke, *Annu. Rev. Cell Dev. Biol.*, 2018, **34**, 495–521.
134 L. K. Wareham, S. A. Liddelow, S. Temple, L. I. Benowitz, A. Di Polo, C. Wellington, J. L. Goldberg, Z. He, X. Duan, G. Bu, A. A. Davis, K. Shekhar, A. La Torre, D. C. Chan, M. V. Canto-Soler, J. G. Flanagan, P. Subramanian, S. Rossi, T. Brunner, D. E. Bovenkamp and D. J. Calkins, *Mol. Neurodegener.*, 2022, **17**, 23.
135 Y. C. Sun, Y. Wan, R. Nam, M. Chu and H. E. Naguib, *Sci. Rep.*, 2019, **9**, 1–13.
136 F. Y. Hsieh, H. H. Lin and S. Hui Hsu, *Biomaterials*, 2015, **71**, 48–57.
137 I. Apsite, G. Constante, M. Dulle, L. Vogt, A. Caspari, A. R. Boccaccini, A. Synytska, S. Salehi and L. Ionov, *Biofabrication*, 2020, **12**, 035027.
138 S. Da Wu and S. H. Hsu, *Biofabrication*, 2021, **13**, 045029.
139 Z. Atoufi, P. Zarrintaj, G. H. Motlagh, A. Amiri, Z. Bagher and S. K. Kamrava, *J. Biomater. Sci., Polym. Ed.*, 2017, **28**, 1617–1638.
140 G. Li, Y. Kong, Y. Zhao, Y. Zhao, L. Zhang and Y. Yang, *J. Biomater. Sci., Polym. Ed.*, 2015, **26**, 899–916.
141 S.-H. Hsiao and S. Hsu, *ACS Appl. Mater. Interfaces*, 2018, **10**, 29273–29287.
142 J. Liu, O. Erol, A. Pantula, W. Liu, Z. Jiang, K. Kobayashi, D. Chatterjee, N. Hibino, L. H. Romer, S. H. Kang, T. D. Nguyen and D. H. Gracias, *ACS Appl. Mater. Interfaces*, 2019, **11**, 8492–8498.
143 D. W. Hutmacher, *Biomaterials*, 2000, **21**, 2529–2543.
144 B. D. Boyan, C. H. Lohmann, J. Romero and Z. Schwartz, *Clin. Plast. Surg.*, 1999, **26**, 629–645.
145 A. Ding, S.-J. Lee, R. Tang, K. L. Gasvoda, F. He and E. Alsberg, *Small*, 2022, **18**, 2202196.
146 A. Ding, O. Jeon, D. Cleveland, K. L. Gasvoda, D. Wells, S.-J. Lee and E. Alsberg, *Adv. Mater.*, 2022, **34**, 2109394.
147 P. J. Díaz-Payno, M. Kalogeropoulou, I. Muntz, E. Kingma, N. Kops, M. D'Este, G. H. Koenderink, L. E. Fratila-Apachitei, G. J. V. M. van Osch and A. A. Zadpoor, *Adv. Healthcare Mater.*, 2023, **12**, 2201891.
148 R. Jamaledin, C. Di Natale, V. Onesto, Z. Taraghdari, E. Zare, P. Makvandi, R. Vecchione and P. Netti, *J. Clin. Med.*, 2020, **9**, 542.
149 J. Goole and K. Amighi, *Int. J. Pharm.*, 2016, **499**, 376–394.
150 J. Firth, A. W. Basit and S. Gaisford, *3D Printing of Pharmaceuticals*, 2018, pp. 133–151.
151 Y. C. Li, Y. S. Zhang, A. Akpek, S. R. Shin and A. Khademhosseini, *Biofabrication*, 2016, **9**, 012001.
152 I. Lukin, S. Musquiz, I. Erezuma, T. H. Al-Tel, N. Golafshan, A. Dolatshahi-Pirouz and G. Orive, *Expert Opin. Drug Discovery*, 2019, **14**, 953–956.
153 J. Li and D. J. Mooney, *Nat. Rev. Mater.*, 2016, **1**, 16071.
154 U. Bozuyuk, O. Yasa, I. C. Yasa, H. Ceylan, S. Kizilel and M. Sitti, *ACS Nano*, 2018, **12**, 9617–9625.
155 M. K. Gupta, F. Meng, B. N. Johnson, Y. L. Kong, L. Tian, Y. W. Yeh, N. Masters, S. Singamaneni and M. C. McAlpine, *Nano Lett.*, 2015, **15**, 5321–5329.
156 K. Malachowski, J. Breger, H. R. Kwag, M. O. Wang, J. P. Fisher, F. M. Selaru and D. H. Gracias, *Angew. Chem., Int. Ed.*, 2014, **53**, 8045–8049.
157 S. Zu, Z. Wang, S. Zhang, Y. Guo, C. Chen, Q. Zhang, Z. Wang, T. Liu, Q. Liu and Z. Zhang, *Mater. Today Chem.*, 2022, **24**, 100789.
158 Q. Hu, P. S. Katti and Z. Gu, *Nanoscale*, 2014, **6**, 12273–12286.
159 H. Ceylan, I. C. Yasa, O. Yasa, A. F. Tabak, J. Giltinan and M. Sitti, *ACS Nano*, 2019, **13**, 3353–3362.
160 H. Li, G. Go, S. Y. Ko, J.-O. Park and S. Park, *Smart Mater. Struct.*, 2016, **25**, 027001.
161 G. Villar, A. J. Heron and H. Bayley, *Nat. Nanotechnol.*, 2011, **6**, 803–808.
162 Y.-D. Zhao, J.-H. Lai and M. Wang, *Nano Life*, 2021, **11**, 2141001.

163 K. Sadtler, A. Singh, M. T. Wolf, X. Wang, D. M. Pardoll and J. H. Elisseeff, *Nat. Rev. Mater.*, 2016, **1**, 1–17.
164 K. Osouli-Bostanabad, T. Masalehdan, R. M. I. Kapsa, A. Quigley, A. Lalatsa, K. F. Bruggeman, S. J. Franks, R. J. Williams and D. R. Nisbet, *ACS Biomater. Sci. Eng.*, 2022, **8**, 2764–2797.
165 L. Faber, A. Yau and Y. Chen, *Biofabrication*, 2013, **16**, 012001.
166 A. Sheikh, M. A. S. Abourehab and P. Kesharwani, *Drug Discovery Today*, 2023, **28**, 1–15.
167 W. Zhou, Z. Qiao, E. Nazarzadeh Zare, J. Huang, X. Zheng, X. Sun, M. Shao, H. Wang, X. Wang, D. Chen, J. Zheng, S. Fang, Y. M. Li, X. Zhang, L. Yang, P. Makvandi and A. Wu, *J. Med. Chem.*, 2020, **63**, 8003–8024.
168 T. R. Hoare and D. S. Kohane, *Polymer*, 2008, **49**, 1993–2007.
169 S. Choudhury, A. Joshi, D. Dasgupta, A. Ghosh, S. Asthana and K. Chatterjee, *Mater. Adv.*, 2024, **5**, 3345–3356.
170 S. Choudhury, A. Joshi, V. Baghel, G. K. Ananthasuresh, S. Asthana, S. Homer-Vanniasinkam and K. Chatterjee, *J. Mater. Chem. B*, 2024, DOI: **10.1039/D4TB00437J**.
171 A. Joshi, S. Choudhury, S. Asthana, S. Homer-Vanniasinkam, U. Nambiar and K. Chatterjee, *Biomater. Sci.*, 2023, **11**, 7703–7708.